ENVISAT GOMOS Monthly report: January/February 2005

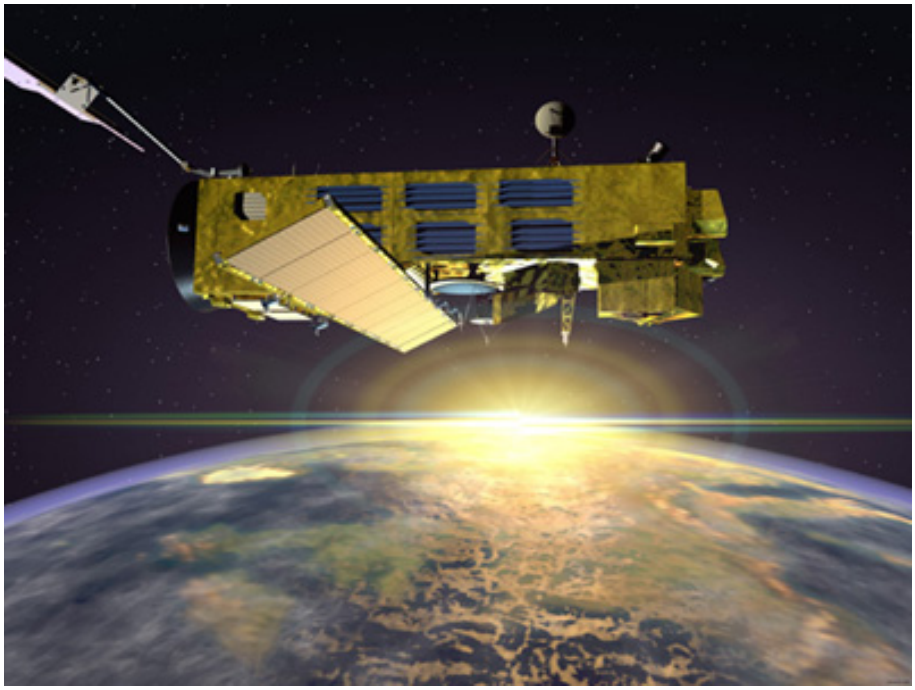

Prepared by:	L. Saavedra de Miguel (PCF Team – EOP/GOQ)
Inputs from:	GOMOS Quality Working Group, ECMWF, ACVT
Issue:	1.0
Reference:	ENVI-SPPA-EOPG-TN-05-0007
Date of issue:	31 March 2005
Status:	Reviewed
Document type:	Technical Note
Approved by:	Rob Koopman

TABLE OF CONTENTS

1 INTRODUCTION

The GOMOS monthly report documents the current status and recent changes to the GOMOS instrument, its data processing chain, and its data products.
The Monthly Report (hereafter MR) is composed of analysis results obtained by the Product Control Facility, combined with inputs received from the different entities working on GOMOS operation, calibration, product validation and data quality. These teams participate in the GOMOS Quality Working Group:

- European Space Agency (ESRIN-PCF, ESOC, ESTEC-PLSO)
- ACRI
- Service d'Aeronomie
- Finnish Meteorological Institute
- IASB-Belgian Institute for Space Aeronomy
- Astrium Space
- ECMWF

In addition, the group interfaces with the Atmospheric Chemistry Validation Team.

1.1 Scope

The main objective of the Monthly Report is to give, on a regular basis, the status of GOMOS instrument performance, data acquisition, results of anomaly investigations, calibration activities and validation campaigns. The following six sections compose the MR:

- Summary
- Unavailability
- Instrument Performance and Configuration
- Level 1 Product Quality Monitoring
- Level 2 Product Quality Monitoring
- Validation Activities and Results

1.2 References

[1] ENVISAT Weekly Mission Operations Report #134, #135, #136, #137 ENVI-ESOC-OPS-RP-1011-TOS-OF
[2] 'Level 1b Detailed Processing Model', PO-RS-ACR-GS-0001, issue 6.1, 28 Nov, 2003
[3] 'Level 2 Detailed Processing Model', PO-RS-ACR-GS-0002, issue 6.0, 6 Feb, 2004
[4] ECMWF GOMOS Monthly Reports
[5] 'Technical Assistance to ENVISAT Validation by LIDAR', Annual report 2004, Yasjka Meijer and Daan Swart (RIVM)

1.3 Acronyms and Abbreviations

ACVT	Atmospheric Chemistry Validation Team
ADF	Auxiliary Data File
ADS	Auxiliary Data Server
ANX	Ascending Node Crossing
ARF	Archiving Facility (PDS)
CCU	Central Communication Unit
CFS	CCU Flight Software
CNES	Centre National d'Études Spatiales
CTI	Configuration Table Interface / Configurable Transfer Item
CR	Cyclic Report
DC	Dark Charge
DMOP	Detailed Mission Operation Plan
DPM	Detailed Processing Model
DS	Data Server
DSA	Dark Sky Area
DSD	Data Set Descriptor
ECMWF	European Centre for Medium Weather Forecast
EQSOL	Equipment Switch Off Line
ESA	European Space Agency
ESL	Expert Support Laboratory
ESRIN	European Space Research Institute
ESTEC	European Space Research & Technology Centre
ESOC	European Space Operations Centre
FCM	Fine Control Mode
FMI	Finnish Meteorological Institute
FOCC	Flight Operations Control Centre (ENVISAT)
FP1	Fast Photometer 1
FP2	Fast Photometer 2
GADS	Global Annotations Data Set
GOMOS	Global Ozone Monitoring by Occultation of Stars
GOPR	GOmos PRototype
GS	Ground Segment
HK	Housekeeping
IASB	Institut d'Aeronomie Spatiale de Belgique
IAT	Interactive Analysis Tool
ICU	Instrument Control Unit
IDL	Interactive Data Language
IECF	Instrument Engineering and Calibration Facilities
IMK	Institute of Meteorology Karlsruhe (Meteorologisch Institut Karlsuhe)
INV	Inventory Facilities (PDS)
IPF	Instrument Processing Facilities (PDS)
JPL	Jet Propulsion Laboratory
LAN	Local Area Network
LMA	Levenberg-Marquardt Algorithm
LPCE	Laboratoire de Physique et Chimie de l'Environnement
LUT	Look Up Table

MCMD	Macro Command
MDE	Mechanism Drive Electronics
MIP	Most Illuminated Pixel
MPH	Main Product Header
MPS	Mission Planning System
MR	Monthly Report
OBT	On Board Time
OCM	Orbit Control Manoeuvre
OOP	Out-of-plane
OP	Operational Phase of ENVISAT
PAC	Processing and Archiving Centre (PDS)
PCF	Product Control Facility
PDCC	Payload Data Control Centre (PDS)
PDHS	Payload Data Handling Station (PDS)
PDHS-E	Payload Data Handling Station – ESRIN
PDHS-K	Payload Data Handling Station – Kiruna
PDS	Payload Data Segment
PEB	Payload Equipment Bay
PLSOL	Payload Switch off Line
PMC	Payload Module Computer
PRNU	Pixel Response Non Uniformity
PSO	On-Orbit Position
QC	Quality Control
QUARC	Quality Analysis and Reporting Computer
QWG	Quality Working Group
RIVM	Rijksinstituut voor Volksgezondheid en Milieu
RTS	Random Telegraphic Signal
SA	Service d'Aeronomie
SAA	South Atlantic Anomaly
SATU	Star Acquisition and Tracking Unit
SFA	Steering Front Assembly
SFCM	Stellar Fine Control Mode
SFM	Steering Front Mechanism
SMNA	Servicio Meteorológico Nacional de Argentina
SODAP	Switch On and Data Acquisition Phase
SPA1	Spectrometer A CCD 1
SPA2	Spectrometer A CCD 2
SPB1	Spectrometer B CCD 1
SPB2	Spectrometer B CCD 2
SPH	Specific Product Header
SQADS	Summary Quality Annotation Data Set
SSP	Sun Shade Position
SZA	Solar Zenith Angle

2 SUMMARY

The GOMOS data measurements are suspended since 24th January 2005, following a major instrument anomaly: the instrument entered in Standby/Refuse mode due to a "Voice_coil_command_saturation" failure, which means that the current computed for the ELEVATION voice coil has been saturated for 10 consecutive cycles. The anomaly re-occurred again after two recovery attempts on January and after some successful testing (no anomaly) performed on 22nd February using fictive star occultations, it was decided to resume the measurement mode. On 3rd March GOMOS started to work nominally before the anomaly occurred after approximately 30 hours of operation, showing the intermittent behavior of this failure. At this point, it was decided to leave the instrument in HEATER mode in order to keep the GOMOS temperature to their operational values (see section 3.1 for more details on the anomaly occurrences). The preliminary investigations point to a mechanical-electrical degradation of the Steering Front Mechanism, affecting the coarse rallying for the star centering. The anomaly investigations proceed, involving the ESA teams at ESTEC, ESOC and ESRIN, together with the GOMOS instrument prime contractor, EADS Astrium (section 3.1).

The level 0 availability is higher than 97% during the reporting period. For level 1 data there is an increasing trend after a peak (72%) on the week 13-19 December 2004. The availability on the third week of January 2005 arrives to 88% (section 3.3).

The detector temperatures during January are one degree greater than the ones registered during the same period in 2004 (global increase due to the radiator ageing). The expected seasonal variation of the temperatures with amplitude of around one degree can be clearly observed. The peaks that occur mainly in spectrometer B1 and B2 are also to be noted. The decrease observed on 25th January 2005 in all detectors is after the GOMOS switch off period, when the instrument did not have enough time to reach the nominal temperature before starting the measurements (section 4.2).

The radiometric sensitivity monitoring shows values outside the warning threshold set to 10% for the photometers. The products with photometer signal that caused the high peaks have been studied in depth and a comparison has been performed between these signals and nominal photometer signals of the same stars. It can be observed that the signals are very high with respect to nominal photometer signals. Apparently, the missing packets at the beginning of the occultations have created a problem in the photometer unfolding algorithm. Investigations are ongoing at this time to find this suspected bug in the algorithm. For star 25, also the UV ratio is greater than 10% and it is clear that there is a global decrease of UV ratios for all the stars. This confirms the expected degradation suffered by the UV optics that is, anyway, very small considering also the small variation for the rest of the stars (section 5.4.1).

On 10th, 17th and 26th January new calibration ADF's were disseminated with updated DC maps of orbits 14622, 14966 and 15177 respectively (section 5.1.2).

3 INSTRUMENT UNAVAILABILITY

3.1 GOMOS Unavailability Periods

In table 3.1-1 there is a list of GOMOS unavailability reports issued during the period 1st January until 5th March 2005. During the reporting period GOMOS was not in measure mode mainly due a major failure.

On 24th January 2004 at 13:47 GOMOS instrument entered in Standby/Refuse mode due to a "Voice_coil_command_saturation" failure, which means that the current computed for the ELEVATION voice coil has been saturated for 10 consecutive cycles. The anomaly occurred during the coarse rallying phase when the mirror was trying to reach star id number 8. The instrument was recovered to measurement on 25th January 2005 but after 40 minutes of operations it entered again in Standby/Refuse mode due to the same anomaly during the coarse rallying phase. The following sequence of measurements could not take place before some hours after the last anomaly occurrence (occultations schedule constraints) so, in order to take advantage of the situation, it was decided to switch off GOMOS and uplink a patch which was "waiting" for a GOMOS switch off occurrence to be up linked. Unfortunately, during the operational procedure to be followed before resume the measurement mode, the instrument entered again in Standby/Refuse mode due to the same anomaly. Some tests were performed on 22 February using fictive star occultations in order to check eventual dependencies of the anomaly on elevation and/or azimuth angles. The tests were performed successfully without any anomaly occurrence but after the recovery of the instrument (3rd March) to measurement mode, the anomaly occurred again showing the intermittent behavior of this failure. At this time, the instrument was left in HEATER mode in order to keep the GOMOS temperature to their operational values. The operations will not continue until further notice. Preliminary investigations point to a mechanical-electrical degradation of the Steering Front Mechanism, affecting the coarse rallying for the star centering.

There were also two small unavailability periods due to satellite manoeuvres (table 3.1-1).

Table 3.1-1: List of unavailability periods issued during the reporting month

Reference of unavailability report	Start time Star orbit	Stop time Stop orbit	Description
EN-UNA-2005/0005	7 Jan 2005 03:00:00.000 Orbit = 14930	7 Jan 2005 13:00:00.000 Orbit = 14936	Planned OCM
EN-UNA-2005/0006	5 Jan 2005 21:44:00.000 Orbit = 14913	6 Jan 2005 00:59:18.000 Orbit = 14915	Planned SFCM
EN-UNA-2005/0025	24 Jan 2005 13:47:03.000 Orbit = 15180	25 Jan 2005 22:50:18.000 Orbit = 15200	GOMOS in STANDBY/REFUSE due to VOICE COIL COMMAND saturation
EN-UNA-2005/0064	25 Jan 2005 23:33:56.000 Orbit = 15200	3 Mar 2005 23:26:01.000 Orbit = 15730	GOMOS in STANDBY/REFUSE due to VCOIL CMDSAT
EN-UNA-2005/0068	5 Mar 2005 05:01:35.000 Orbit = 15747	Further notice	GOMOS is in standby/refuse mode owing to VCOIL CMDSAT

3.2 Stars Lost in Centering

The acquisition of a star initiates with a rallying phase where the telescope mechanism is directed towards the expected position of the star. Subsequently the acquisition procedure enters into detection mode, where the SATU star tracker output signal is pre-processed for spot presence survey and for the location of the most illuminated couple of adjacent pixels for two added lines, over the detection field. The Most Illuminated Pixel (MIP) defines the position of the first SATU centering window. The next step in the acquisition sequence is then initiated and consists of a centering phase where the SATU output signal is pre-processed for spot presence survey over the maximum of 10x10 pixel field. This allows the third phase to begin: the tracking phase. The centering phase has occasionally resulted in loss of the star from the field of view. The fig. 3.2-1 reports the percentage of the stars lost in centering for the period

03-FEB-2003 to 23-JAN-2005. It can be seen that three stars, mainly weak stars (higher star id means higher magnitude) are lost during centering phase between 5 and 6 % of their planned observations. The star id 115 was lost 40% of the times but it was planned to be occulted five times and was lost twice (in period 26th January – 1st February 2004), so this high percentage of loss is not statistically significant.

As the monitoring shows neither trend nor excessively high percentages of loss, there is no need for the moment to reject any star from the catalogue, and there is no indication of instrument-related problems.

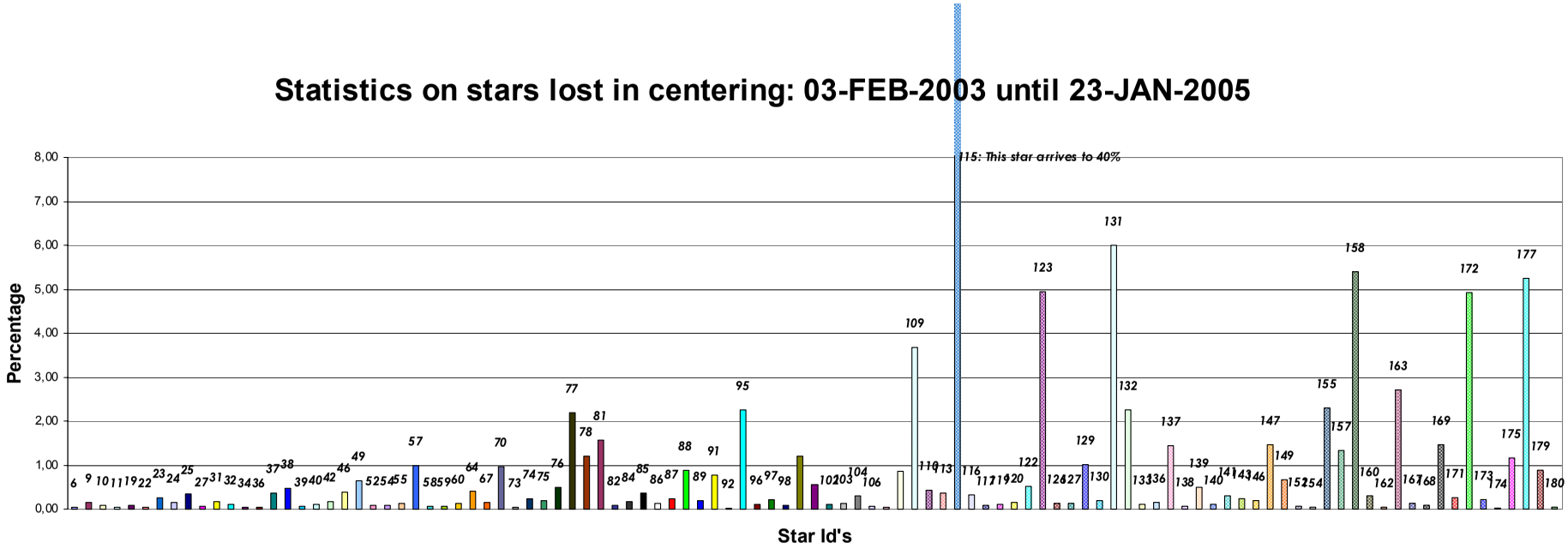

Figure 3.2-1: Statistics on stars that have been lost during the centering phase. The number above the columns correspond to the Star I

3.3 Data Generation Gaps

The trend in percentage of available data within the archives PDHS-K and PDHS-E is depicted in fig. 3.3-1 (when instrument was in operation). It is a good indicator on how the PDS chain is working in terms of generation and dissemination of data to the archives. The percentage is calculated once per week.

The level 0 availability is higher than 97% during the reporting period. For level 1 data there is an increasing trend after a peak (72%) on the week 13-19 December 2004. The availability on the third week of January 2005 arrives to 88%.

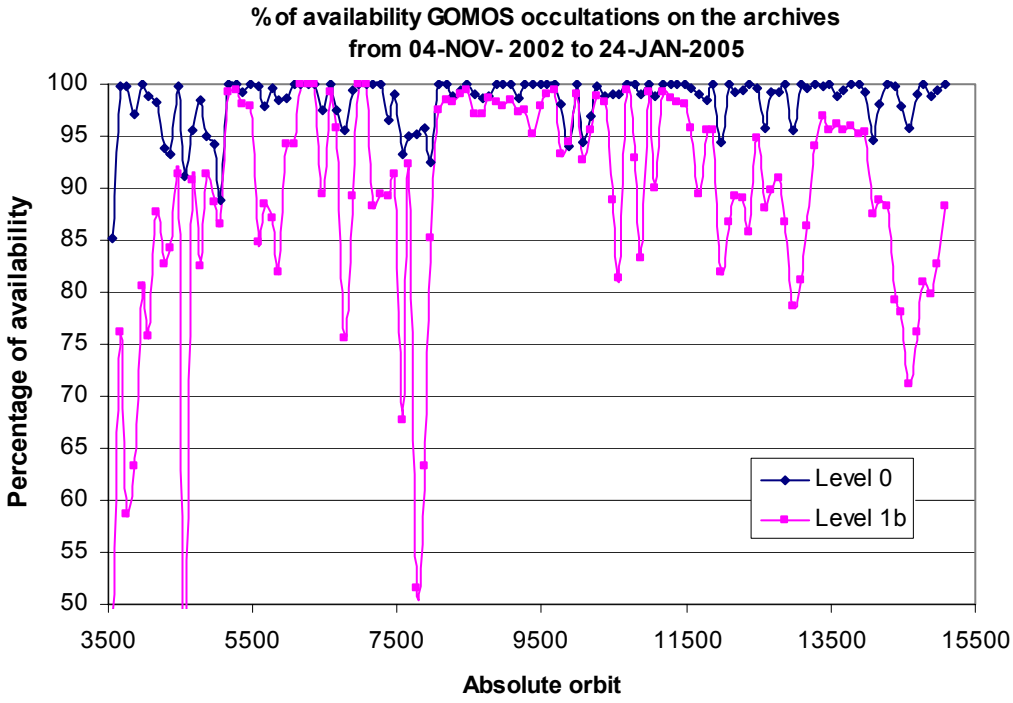

Figure 3.3-1: Percentage of level 0 and level 1b data availability on the archives PDHS-E and PDHS-K

3.3.1 LEVEL 0 PRODUCTS: GOM_NL__0P

Occultations planned to be acquired but for which no GOM_NL__0P data product has become available are presented in fig. 3.3-2 for the reporting period.

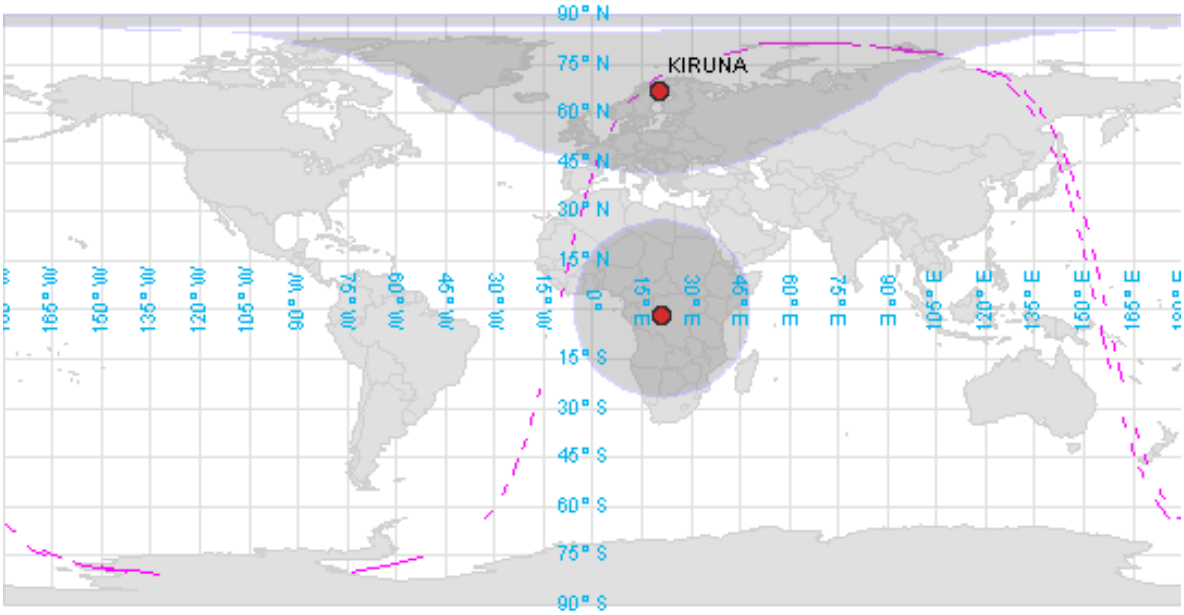

Figure 3.3-2: The pink lines are the orbit segments corresponding to planned data acquisitions for which no GOMOS level 0 product has become available. The grey shadow centered in Kiruna represents the visibility of that ground station. The grey shadow centered in Africa represents ARTEMIS satellite nominal position

3.3.2 HIGHER LEVEL PRODUCTS

Routine dissemination of higher-level products produced by the PDS to Cal/Val teams and other users is enabled. Currently ESA is also providing products from 2003 that are reprocessed with the last version of the prototype processor developed and operated by ACRI.

4 INSTRUMENT CONFIGURATION AND PERFORMANCE

4.1 Instrument Operation and Configuration

The instrument is not in operations since 24th January 2005 as explained in section 3.1.

During the period end of March 2003 to July 2003 the azimuth range had to be decreased in steps (table 4.1-1) to avoid an instrument problem ("Voice_coil_command_saturation" anomaly) that caused GOMOS to go into STAND BY/REFUSE mode. On July 2003 the driver assembly was switched to the redundant B-side and since that date the full azimuth range (-10.8, +90.8) is again available.

Table 4.1-1: Historical changes in Azimuth configuration

Date	Orbit	Minimum Azimuth	Maximum Azimuth
29-MAR-2003 17:40	5635	0.0	+90.8
31-MAY-2003 06:22	6530	+4.0	+90.8

16-JUN-2003 16:17	6765	+12.0	+90.8
15-JUL-2003 01:39	7200	-10.8	+90.8

The operations of the instrument in other modes than occultation mode are identified in table 4.1-2. For the reporting month, there were neither operation in calibration mode not DSA observations planned.

There was no new Configurable Table Interface (CTI) uploaded to the instrument. The files used since the beginning of the mission are in table 4.1-3.

Table 4.1-2: GOMOS operations during the reporting period

UTC time	Start orbit	Stop orbit	Mode (Asynchronous or Synchronous)	Calibration (CAL) or Dark Sky Area (DSA)
-	-	-	-	-

Table 4.1-3: Historic CTI Tables

CTI filename	Dissemination to FOCC
CTI_SMP_GMVIEC20030716_123904_00000000_00000004_20030715_000000_20781231_235959.N1	16-JUL-2003
CTI_SMP_GMVIEC20021104_075734_00000000_00000003_20021002_000000_20781231_235959.N1	06-NOV-2003
CTI_SMP_GMVIEC20021002_082339_00000000_00000002_20021002_000000_20781231_235959.N1	07-OCT-2003
CTI_SMP_GMVIEC20020207_154455_00000000_00000000_20020301_032709_20781231_235959.N1	21-FEB-2002

4.2 Limb, Illumination conditions and instrument gain setting

The **limb** and the **illumination condition** are two parameters that can confuse the user community. In table 4.2-1 there are specified the product (level 1b and level 2) parameter where the flag is located, the meaning and the source. The difference between the limb (SPH/bright_limb) and the illumination condition (SUMMARY_QUALITY/limb_flag) is that the first one is coming from the mission scenario and the second is coming from the processing (sun zenith angle computed). The SPH/bright_limb is for some occultations set to “dark” in the mission scenario while they are in fact in bright limb illumination conditions.

Table 4.2-1: Relationship between limb, illumination condition flags and instrument gain settings

Products parameter	SPH/bright_limb	0 = Dark	1 = Bright	Coming from mission scenario
	SUMMARY_QUALITY/limb_flag	0 = Full Dark 1 = Bright 2 = Twilight	1 = Bright 2 = Twilight	In the geolocation process the sun zenith angle is computed and the occultation then is flagged accordingly
Instrument Gain	SPA Gain	3 (2)	0	Gain setting for spectrometer A. In parenthesis, values valid only for Sirius occultations (starID=1)
	SPB Gain	0	0	Gain setting for spectrometer B

To select highest quality data for scientific application, data with SUMMARY_QUALITY/limb_flag equal to '0' should be used (see also the disclaimer: http://envisat.esa.int/dataproducts/availability/disclaimers). The instrument gain settings are also specified in table 4.2-1 (they depend on the mission scenario flags) just for information completeness.

4.3 Thermal Performance

Since the beginning of the mission the hot pixel and RTS phenomena are producing a continuous increase of the dark charge signal within the CCD detectors (see section 4.5.1). In order to minimize this effect, three successive CCD cool down were performed in orbits 800 (25th April 2002), 1050 (13th May 2002) and 2780 (11th September 2002) with a total decrease in temperature of 14 degrees.

Fig. 4.3-1 and 4.3-2 display, respectively, the overall temperature variation and the temperature variation around the Ascending Node Crossing (ANX) time with a resolution of 0.4 degrees (coding accuracy for level 0 data). The CCD temperatures during January 2005 are one degree greater than the ones registered during the same period in 2004 (global increase due to the radiator ageing). The expected seasonal variation of the temperatures with amplitude of around one degree can be clearly observed. The peaks that occur mainly in spectrometer B1 and B2 are also to be noted. They happen for some consecutive orbits and every 8-10 days. Their origin is still not known, as we did not find any correlation between these peaks and other activities carried out by other ENVISAT instruments. The CCD temperature at almost the same latitude location (fig. 4.3-2) is monitored in order to detect any inter-orbital temperature variation.

The decrease observed on 24th March 2003, twice in September 2003, at the beginning of December 2003 and on January 2005 in all detectors is after GOMOS switch off periods, when the instrument did not have enough time to reach the nominal temperature before starting the measurements.

The orbital temperature variation of the detector SPB2 (fig. 4.3-3 & 4.3-4) is around 3.3 degrees, slightly higher than nominal (2-2.5 degrees) due to the GOMOS switch off. The stability of the temperature during the orbit is important because it affects the position of the interference patterns. The phenomenon of the interference is present mainly in SPB and this Pixel Response Non-Uniformity (PRNU) is corrected during the processing.

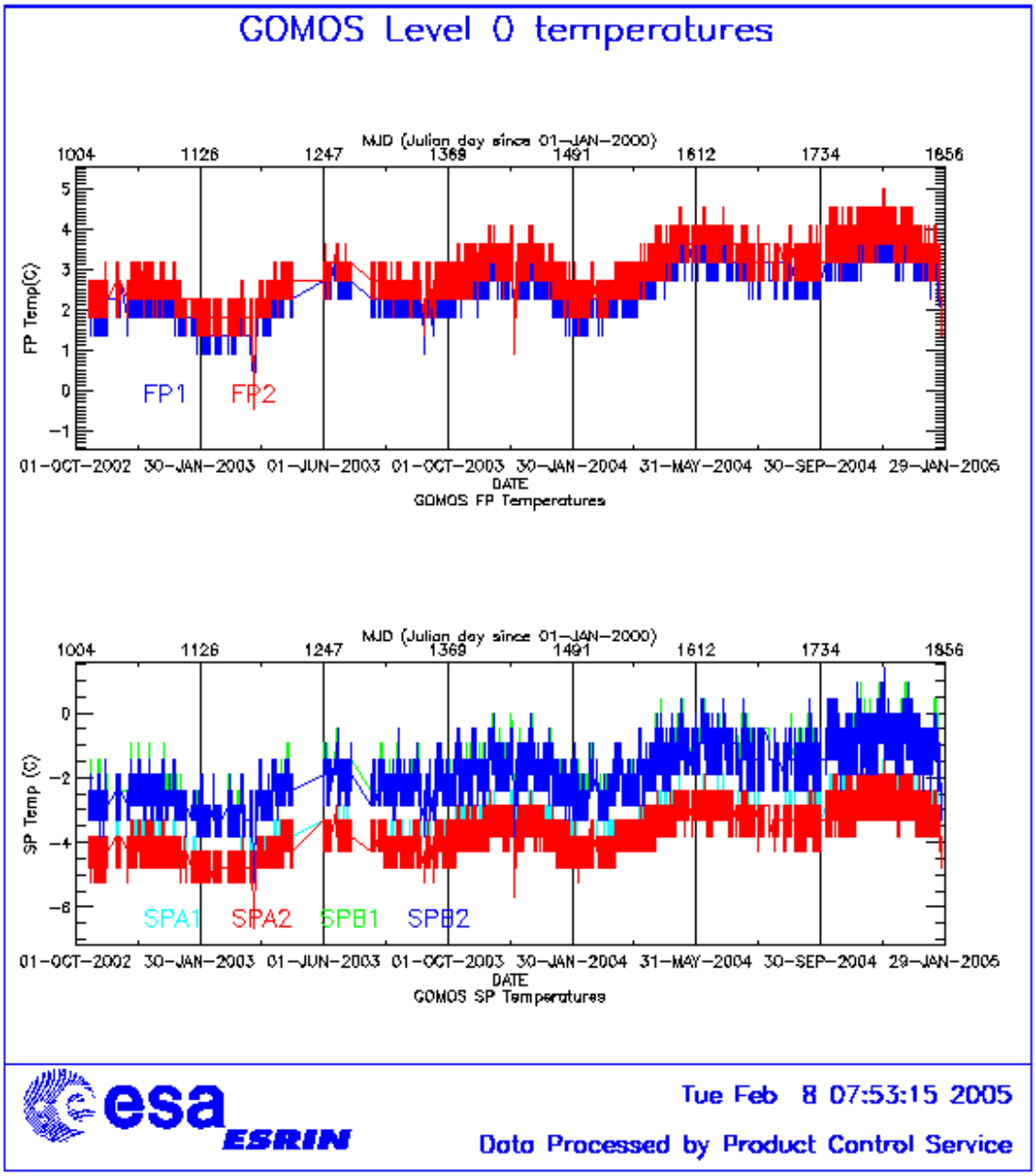

Figure 4.3-1: Level 0 temperature evolution of all GOMOS CCD detectors since October 2002 until the end of the reporting period

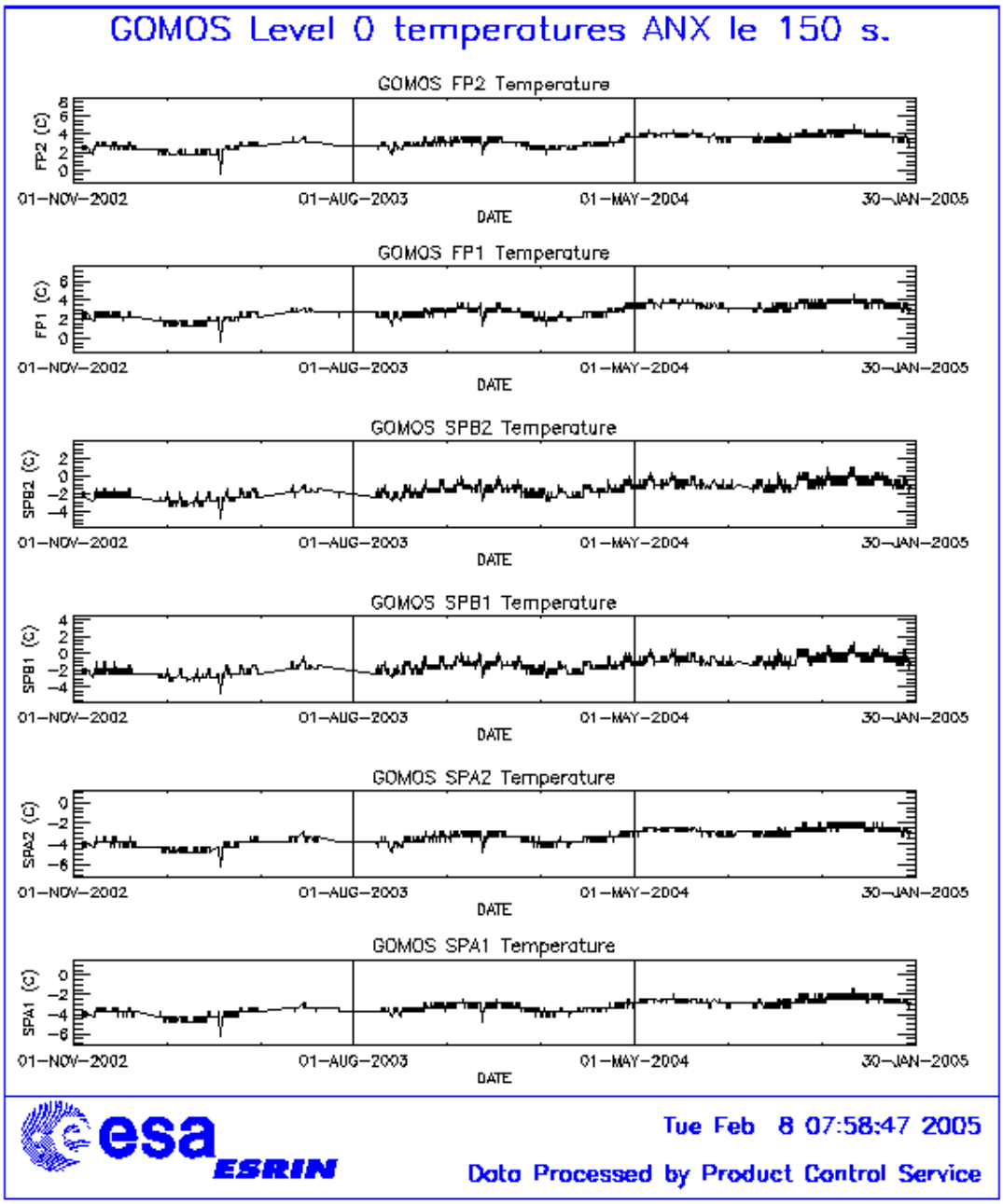

Figure 4.3-2: **Level 0 temperature evolution of all GOMOS CCD detectors around ANX since November 2002 until the end of the reporting period**

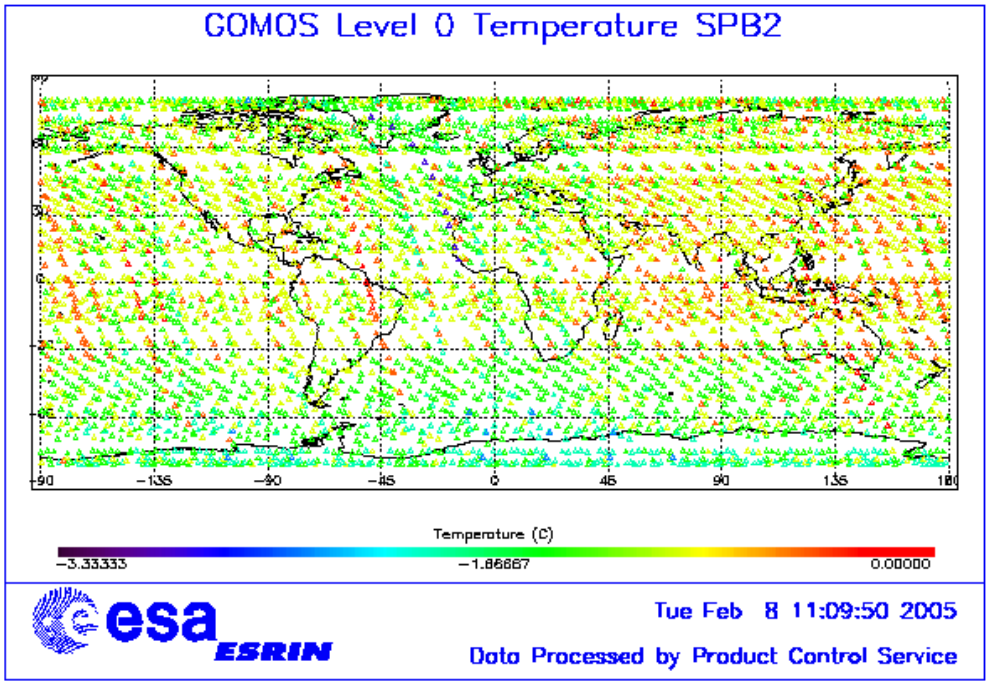

Figure 4.3-3: Ascending orbital variation of SPB2 temperature during reporting period

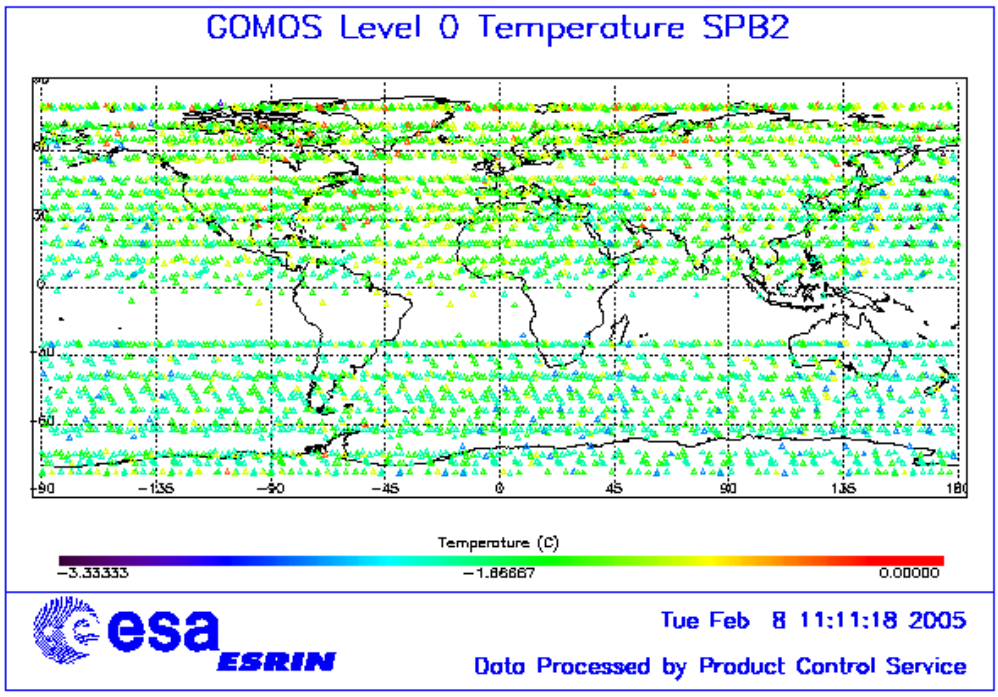

Figure 4.3-4: Descending orbital variation of SPB2 temperature during reporting period

4.4 Optomechanical Performance

No new band setting calibration has been performed during the reporting period. The last one has been done on December 2004.

- Version GOMOS/4.00 and previous ones:

In the processors versions of GOMOS GOMOS/4.00 and previous the spectra is expected to be aligned along CCD lines, and therefore use only a single average line index per CCD. In table 4.4-1 the mean values of the location of the star signal for all the calibration analysis done are reported. The 'left' and 'right' values are calculated (the whole interval is not used) because the spectra present a slight slope, more pronounced in the spectrometer B (see fig. 4.4-1). In table 4.4-2, mean values of the location of the star signal are calculated for some specific wavelength intervals. These intervals have been changed between the calibration performed in September 2002 and the ones performed afterwards (until November 2003). Table 4.4-3 reports the average location of the star spot on the photometer 1 and 2 CCD.

- Version GOMOS/4.02:

In the actual processor version (GOMOS/4.02) operational since 23rd March 2004, a Look Up Table (LUT) gives the line index of the spectra location as a function of the wavelength (blue dots in fig. 4.4-1). A new calibration exercise has been performed during December 2004. The position of the stellar spectra of star id 23, 10 and 2 observed in dark-limb spatial spread monitoring mode have been averaged above 120 km altitude and compared to the values of the LUT. The results confirm the LUT values (see table 4.4-4) so for the time being there is no need to update the LUT.

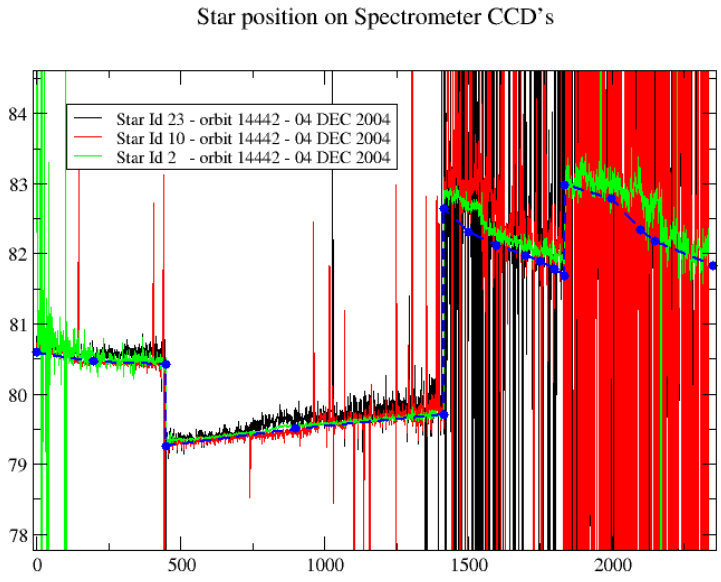

Figure 4.4-1: Average position of star spectra on the CCD

Table 4.4-1: Mean value of the location of the star signal during the occultation at the edges of every band (mean over 50 values, filtering the outliers)

	UV (SPA1) left/right	VIS (SPA2) left/right (Inverted spectra)	IR1 (SPB1) left/right	IR2 (SPB2) left/right
11/09/2002	80.7/80.7	79.8/79.5	82.8/81.9	83.1/82.1
01/01/2003	80.7/80.6	79.8/79.5	82.8/82.0	83.2/82.2
17/07/2003 & 02/08/2003	80.7/80.7	79.8/79.5	82.8/81.9	83.1/82.1
08/11/2003	80.7/80.6	79.8/79.5	82.8/81.9	83.1/82.1

Table 4.4-2: Mean value of the location of the star signal during the occultation (as table 4.4-1) but now within some wavelength intervals

	UV (SPA1)	VIS (SPA2)	IR1 (SPB1)	IR2 (SPB2)
11/09/2002 wl range (nm)	80.8 [300-330]	79.8 [500-530]	82.6 [760-765]	82.9 [937-942]
01/01/2003 wl range (nm)	80.6 [350-360]	78.6 [650-670]	81.6 [760-765]	80.3 [935-945]
02/08/2003	80.6	79.7	82.5	82.8
08/11/2003	80.6	79.9	82.4	82.8

Table 4.4-3: Average column and row pixel location of the star spot on the photometer CCD during the occultation

	FP1 (column/row)	FP2 (column/row)
11/09/2002	11/4	5/5
01/01/2003	10/4	6/4.9
02/08/2003	10/4	6/5
08/11/2003	10/4	6/5
04/12/2004	10/4	6/5

Table 4.4-4: Location of the star signal on the CCD's (corresponding to fig. 4.4-1)

Pixel Column	LUT (Pixel line)	Calibration on 10-APR-2004	Calibration on 04-DEC-2004
0	**80.59**	80.80	80.67
20	**80.46**	80.60	80.44
449	**80.42**	80.50	80.42
450	**79.25**	79.39	79.30
900	**79.50**	79.63	79.57
1415	**79.70**	79.76	79.76
1416	**82.64**	82.80	82.88
1500	**82.31**	82.60	82.66
1600	**82.12**	82.22	82.30
1700	**81.97**	82.04	82.08
1750	**81.89**	81.98	82.03
1800	**81.78**	81.91	81.96
1835	**81.68**	81.88	81.94
1836	**82.98**	83.10	83.10
2000	**82.78**	82.90	82.94
2100	**82.33**	82.70	82.73
2150	**82.17**	82.40	82.54
2350	**81.83**	82.00	82.00

4.5 Electronic Performance

4.5.1 DARK CHARGE EVOLUTION AND TREND

The trend of Dark Charge (DC) is of crucial importance for the final quality of the products, and is therefore subject to intense monitoring. As part of the DC there is:

- "Hot pixels", a pixel is "hot" when its dark charge exceeds its value measured on ground, at the same temperature, by a significant amount.
- RTS phenomenon (Random Telegraphic Signal), it is an abrupt change (positive or negative) of the CCD pixel signal, random in time, affecting only the DC part of the signal and not the photon generated signal.

The temperature dependence of the DC would make this parameter a good indicator of the DC behaviour, but the hot pixels and the RTS are producing a continuous increase of the DC (see trend in fig. 4.5-1 and 4.5-2). To take into account these phenomena, since version GOMOS/4.00 (actual one is GOMOS/4.02) a DC map per orbit is extracted from a Dark Sky Area (DSA) observation performed around ANX (full dark conditions). For every level 1b product (occultation), the actual thermistor temperature of the CCD is used to convert the DC map measured around ANX into an estimate of the DC at the time (and different temperature) of the actual occultation. When the DSA observation is not available, the DC map inside the calibration product that was measured at a given thermistor reference temperature is used; again, the actual thermistor temperature of the CCD is used to compute the actual map. Table 4.5-1 reports the list of products (50 level 1b products per day are monitored) that used the DC maps inside the calibration file due to the non-availability of DSA observation. A "CAL DC map with no T dep." means that, as the temperature information was not available for that occultation, the DC map used is exactly the one inside the Calibration product.

Table 4.5-1: Table of level 1b products that used the Calibration DC maps instead of the DSA observation

Filename	DC information
GOM_TRA_1PNPDE20050101_025215_000000372033_00261_14844_0000.N1	DC map with no T dep.
GOM_TRA_1PNPDE20050104_204005_000000522033_00315_14898_0000.N1	DC map with no T dep.
GOM_TRA_1PNPDE20050104_204221_000000562033_00315_14898_0001.N1	DC map used
GOM_TRA_1PNPDE20050104_204408_000000522033_00315_14898_0002.N1	DC map used
GOM_TRA_1PNPDE20050104_204531_000000472033_00315_14898_0003.N1	DC map used
GOM_TRA_1PNPDE20050104_204728_000000462033_00315_14898_0004.N1	DC map used
GOM_TRA_1PNPDE20050104_205010_000000442033_00315_14898_0005.N1	DC map used
GOM_TRA_1PNPDE20050104_205141_000000412033_00315_14898_0006.N1	DC map used
GOM_TRA_1PNPDE20050104_205403_000000432033_00315_14898_0007.N1	DC map used
GOM_TRA_1PNPDE20050104_205713_000000462033_00315_14898_0008.N1	DC map used
GOM_TRA_1PNPDE20050104_205900_000000442033_00315_14898_0009.N1	DC map used
GOM_TRA_1PNPDE20050104_210125_000000542033_00315_14898_0010.N1	DC map used
GOM_TRA_1PNPDE20050104_210426_000000512033_00315_14898_0011.N1	DC map used
GOM_TRA_1PNPDE20050104_210606_000000462033_00315_14898_0012.N1	DC map used
GOM_TRA_1PNPDE20050104_210729_000000402033_00315_14898_0013.N1	DC map used

GOM_TRA_1PNPDE20050104_210850_000000392033_00315_14898_0014.N1	DC map used
GOM_TRA_1PNPDE20050104_211009_000000402033_00315_14898_0015.N1	DC map used
GOM_TRA_1PNPDE20050104_211224_000000402033_00315_14898_0016.N1	DC map used
GOM_TRA_1PNPDE20050104_211433_000000382033_00315_14898_0017.N1	DC map used
GOM_TRA_1PNPDE20050104_211552_000000382033_00315_14898_0018.N1	DC map used
GOM_TRA_1PNPDE20050104_212438_000000382033_00315_14898_0019.N1	DC map used
GOM_TRA_1PNPDE20050104_212651_000000492033_00315_14898_0020.N1	DC map used
GOM_TRA_1PNPDE20050104_212859_000000352033_00315_14898_0021.N1	DC map used
GOM_TRA_1PNPDE20050104_213052_000000582033_00315_14898_0022.N1	DC map used
GOM_TRA_1PNPDE20050104_213258_000000382033_00315_14898_0023.N1	DC map used
GOM_TRA_1PNPDE20050104_213513_000000342033_00315_14898_0024.N1	DC map used
GOM_TRA_1PNPDE20050104_214008_000000452033_00315_14898_0025.N1	DC map used
GOM_TRA_1PNPDE20050104_214401_000000652033_00315_14898_0026.N1	DC map used
GOM_TRA_1PNPDE20050104_214612_000000352033_00315_14898_0027.N1	DC map used
GOM_TRA_1PNPDE20050104_214835_000000632033_00315_14898_0028.N1	DC map used
GOM_TRA_1PNPDE20050107_204443_000000432033_00358_14941_0000.N1	DC map used
GOM_TRA_1PNPDE20050107_204609_000000502033_00358_14941_0001.N1	DC map used
GOM_TRA_1PNPDE20050107_205004_000000522033_00358_14941_0002.N1	DC map used
GOM_TRA_1PNPDE20050107_205136_000000462033_00358_14941_0003.N1	DC map used
GOM_TRA_1PNPDE20050107_205326_000000462033_00358_14941_0004.N1	DC map used
GOM_TRA_1PNPDE20050107_205606_000000442033_00358_14941_0005.N1	DC map used
GOM_TRA_1PNPDE20050121_011154_000001602034_00045_15129_0000.N1	DC map with no T dep.
GOM_TRA_1PNPDE20050121_011719_000000532034_00045_15129_0001.N1	DC map used
GOM_TRA_1PNPDE20050121_011851_000000452034_00045_15129_0002.N1	DC map used
GOM_TRA_1PNPDE20050121_012442_000000432034_00045_15129_0003.N1	DC map used

In fig. 4.5-1 and 4.5-2 it is plotted the average DC inserted by the processor into the level 1b data products for the spectrometers SPA1 and SPB2 (per band: upper, central and lower). From the figures, it can be seen that the DC is increasing at the expected rate. The decrease observed at the end of the reporting period is related to the temperature decrease.

The same DC values are plotted in fig. 4.5-3 but for some occultations belonging only to the reporting month.

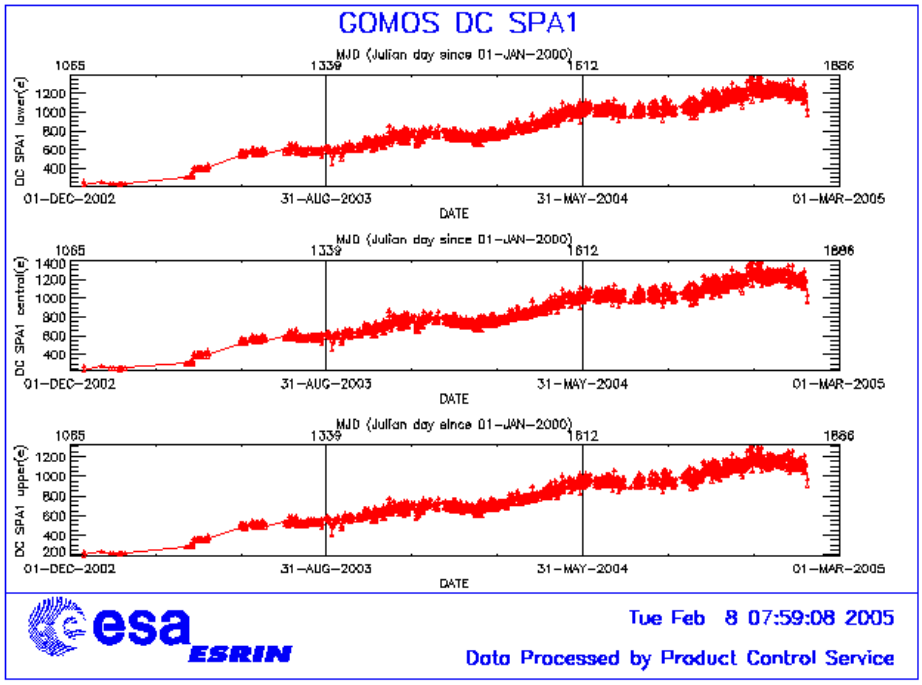

Figure 4.5-1: Mean DC evolution on SPA1 since 15th December 2002 until the end of the reporting period

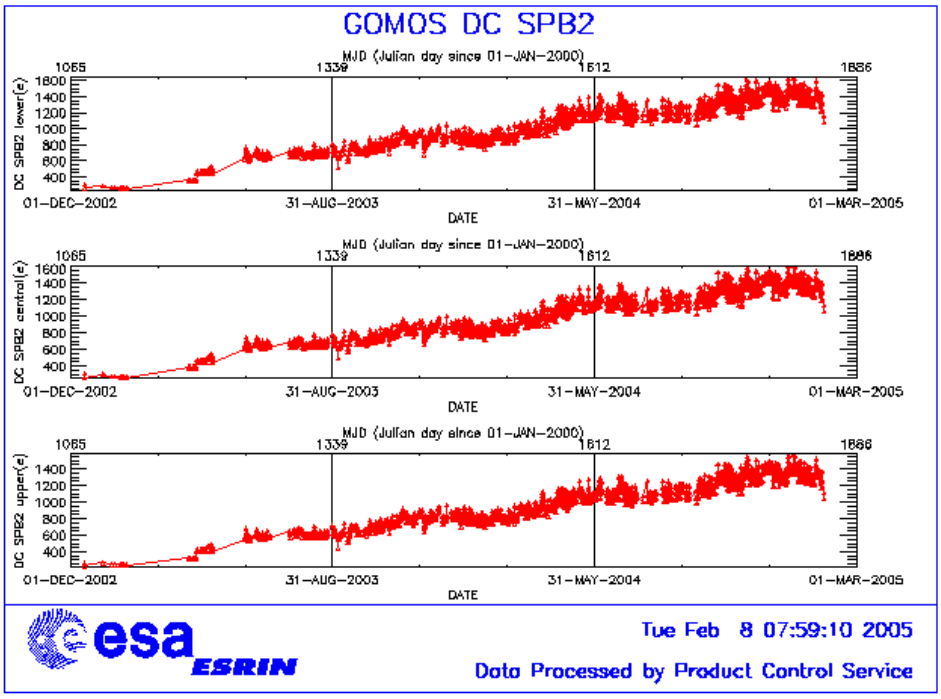

Figure 4.5-2: Mean DC evolution on SPB2 from 15th December 2002 until the end of the reporting period

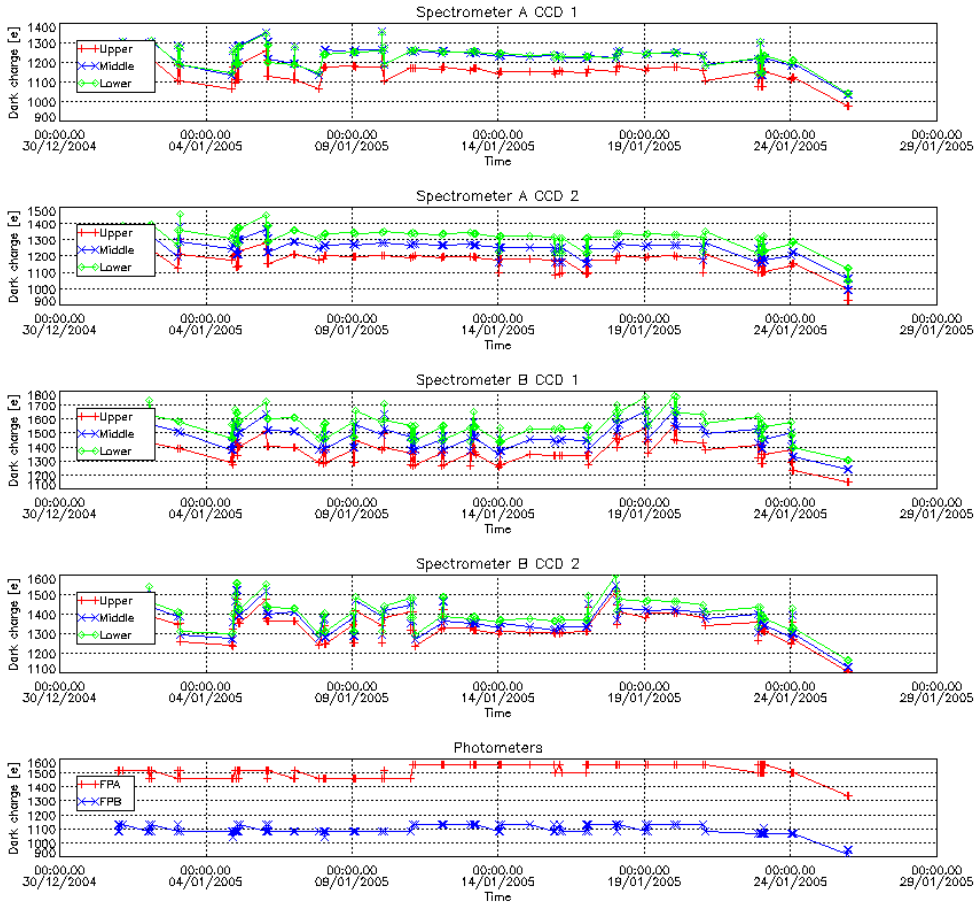

Figure 4.5-3: Mean Dark Charge of spectrometers and photometers during reporting period

4.5.2 SIGNAL MODULATION

A parasitic signal was found to be systematically present, added to the useful signal, at least for spectrometers A1 and A2. The modulation is corrected in the data processing, but the modulation signal standard deviation is routinely monitored in order to detect any trend (fig. 4.5-4).

The modulation standard deviation, for every spectrometer, is characterised as follows:

$$\sigma_{mod} = (\text{'static noises'} - \text{'total static variance'})^{1/2} / \text{gain} \qquad \text{(in ADU)}$$

- The 'static noises' are calculated from the DSA observation performed once per orbit
- The 'total static variance' is obtained from ADF data (electronic chain noise, quantization noise).

The standard deviation of the modulation signal (fig. 4.5-4) presents high values after the inclusion, at the end of March 2004, of the ESRIN level 0 data. It is now confirmed that the South Atlantic Anomaly is the cause of these unexpected peaks. The quality of ESRIN data, in particular over the SAA zone, is thus

under investigation. However, in the second half of October the peaks are smaller because the DSA zone where the data are taking for this analysis is moving towards the Northern Hemisphere. At the end of October the DSA zone is definitely chosen by the planning system in the Northern Hemisphere (to fill the criteria 'DSA in full dark limb conditions') and the high peaks have disappeared.

There is also a very small decreasing trend observed, mainly for SPA1, which for now is not a reason to worry about.

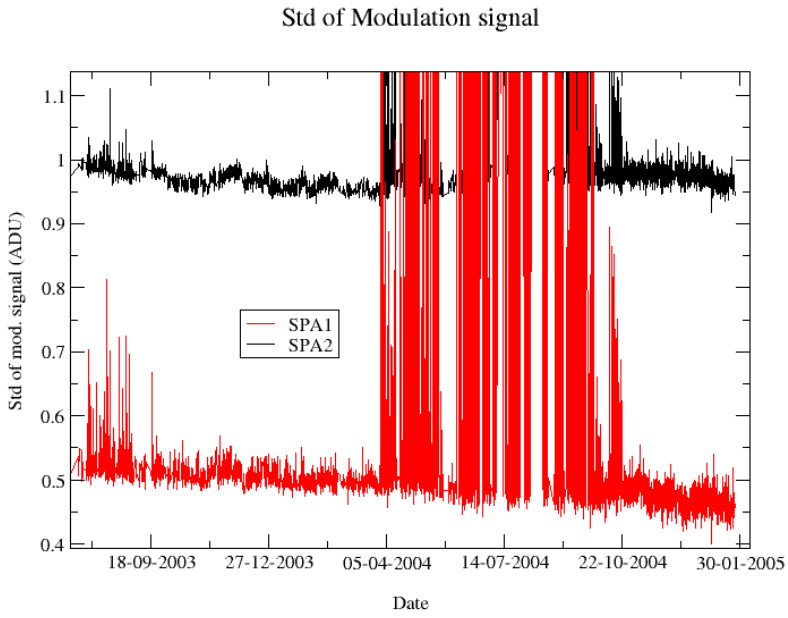

Figure 4.5-4: Standard deviation of the modulation signal

4.5.3 ELECTRONIC CHAIN GAIN AND OFFSET

No new electronic chain gain and offset calibration has been done during the reporting period so these results have been already presented in previous MR.

The routine monitoring of the ADC offset is a good indicator of the ageing of the instrument electronics. During the definition of this routine activity, an exercise has been done to analyze the variation of the ADC offset using the calibration observation in linearity mode (orbits 2810, 4384, 4834, 5219 and 5734). The fig. 4.5-5 presents the evolution of the calibrated ADC offset for each spectrometer electronic chain. The unexpected increase of this offset seems to be due to an external contribution. In the ADC offset calibration procedure, linearity observations are used with two integration times of 0.25 and 0.50 seconds to extrapolate to an integration time of 0 seconds that give the complete chain offset and not only the ADC offset. The complete offset contains any possible offsets, and especially the static dark charge (i.e. the dark charge that does not depend on the spectrometer integration time). If the memory area of the CCD is affected by the generation of hot pixels (this is confirmed by the presence of vertical lines visible in the measurement maps in spatial spread monitoring mode), it becomes that the increase observed in fig. 4.5-5 is due to these new hot pixels.

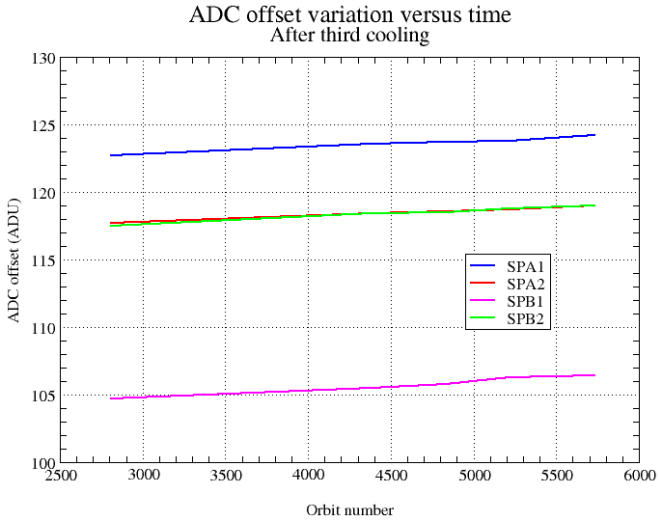

Figure 4.5-5: Evolution of the ADC offset for each spectrometer electronic chain

Next task consists in completing the analysis to confirm that the offset increase is due to the hot pixels in memory area. This can be proven by the study of the noise due to the increased dark charge. The increase of ADC offset will be assumed to be equal to the increase of 'static dark charge' and the corresponding noise will be computed and compared to the increase of the signal variance residual.

If we keep the ADC offset constant, as it is also used to compute the dark charge at band level used to correct the samples in the level 1b processing, the increase of the static dark charge - not taken into account in the ADC offset - is compensated by an artificial increase of the calibrated dark charge. So, the star and limb spectra are correctly corrected for dark charge. A small bias can be added to the instrument noise due to the incorrect dark charge level. Anyway, this quantity is not large enough to require a modification of the ADC offset value.

4.6 Acquisition, Detection and Pointing Performance

4.6.1 SATU NOISE EQUIVALENT ANGLE

The Star Acquisition and Tracking Unit (SATU) noise equivalent angle (SATU NEA) consists of the statistical angular variation of the SATU data above the atmosphere.
The mean of the standard deviation (STD over the 50 values per measurement) above 105 km are computed for every occultation, giving two values per occultation: one in the 'X' direction, one in the 'Y' direction. A mean value per day in every direction and limb is calculated and monitored in order to assess instrument performance in terms of star pointing. The thresholds are 2 and 3 micro radians in 'X' and 'Y' directions respectively. Before May 2003, data above 90 km have been considered (instead of 105 km) but from May 2003 on, data taken in the mesospheric oxygen layer (located around 100 km altitude) have been avoided because they could cause fluctuations on the SATU data. Also the products with errors (error flag set) are discarded from May 2003 onwards.

It can be seen in fig. 4-6.1 that the SATU NEA had some fluctuations during the reporting period but very well below the thresholds.

The results for some occultations belonging to previous months (monthly averages) are presented in fig. 4.6-2, where no trend is visible so far.

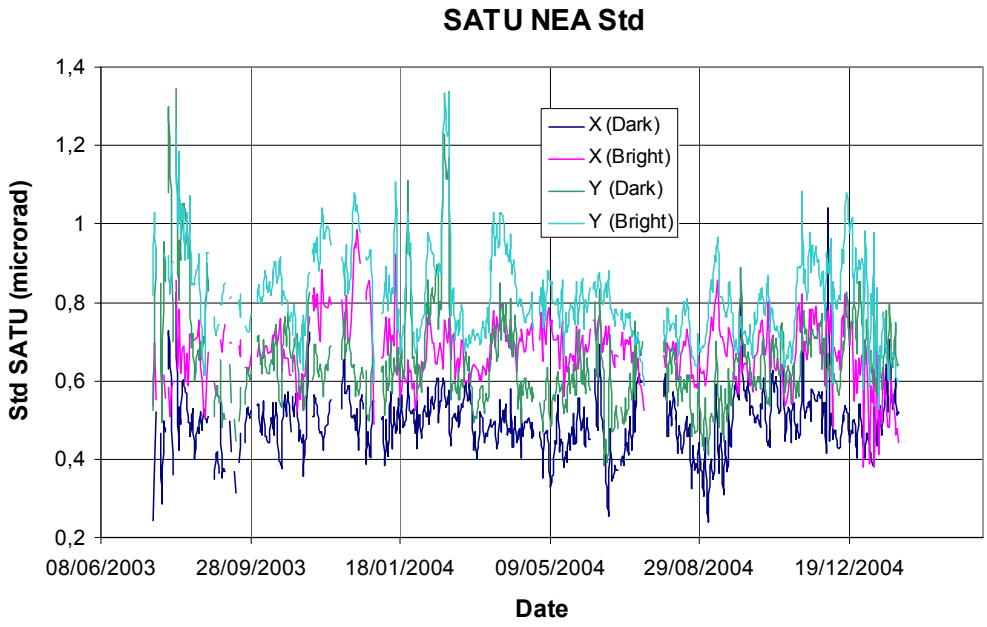

Thresholds:
'X' direction: 2 microrad
'Y' direction: 3 microrad

Figure 4.6-1: Average value per day of SATU NEA STD above 105 km

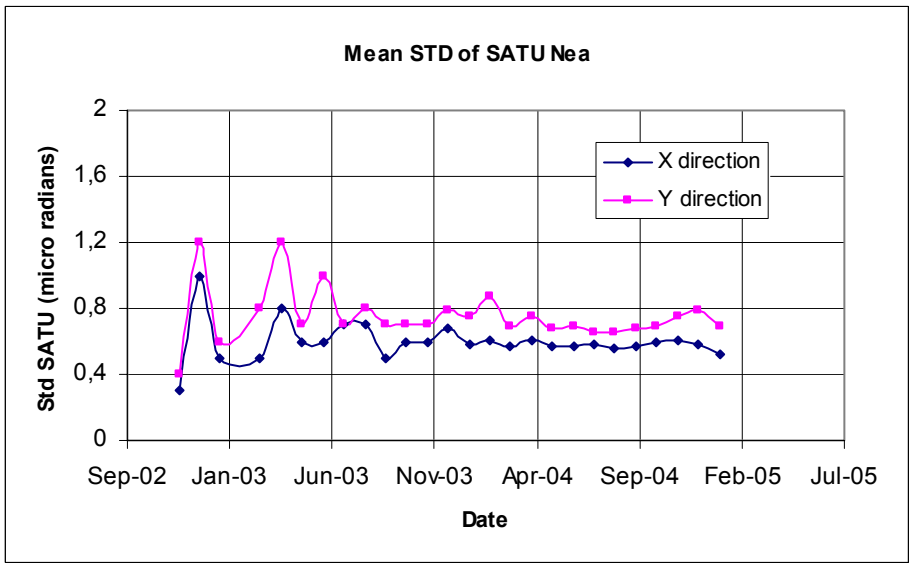

Figure 4.6-2: Average value per month of SATU NEA STD above 105 km

4.6.2 TRACKING LOSS INFORMATION

This verification consists of the monitoring of the tangent altitude at which the star is lost. It is an indicator of the pointing performance although it is to be considered that star tracking is also lost due to the presence of clouds and hence not only due to deficiencies in the pointing performance. Therefore, only the detection of any systematic long-term trend is the main purpose of this monitoring. The recent results are presented in fig. 4.6-3, 4.6-4 and 4.6-5:

- The dependence of the altitude at which tracking is lost on the magnitude of the star is very small because the tracking is mainly lost due to the refraction and the scintillation that depend on the atmospheric conditions.
- There are no stars lost at very high altitude neither in dark nor in bright (fig. 4.6-3 & 4.6-4). In twilight there is a star lost very high because it is a partial occultation at the end of an orbit (fig. 4.6-5).
- Some daily statistics are given in fig. 4.6-6 since October 2003. The high peaks are due to the long lasting occultations or partial occultations (occultations at the end of the orbit, being the entire occultation included within the following orbit). A decreasing trend is detected since December 2004 most probably caused by the fact that there were neither long lasting occultations nor partial occultations within the level 1b dataset used for the monitoring.
- Some monthly statistics are given in fig. 4.6-7 calculated for a set of data and not for the whole months. A decreasing trend is observed for the monthly mean bright tangent altitude lost (see previous bullet).

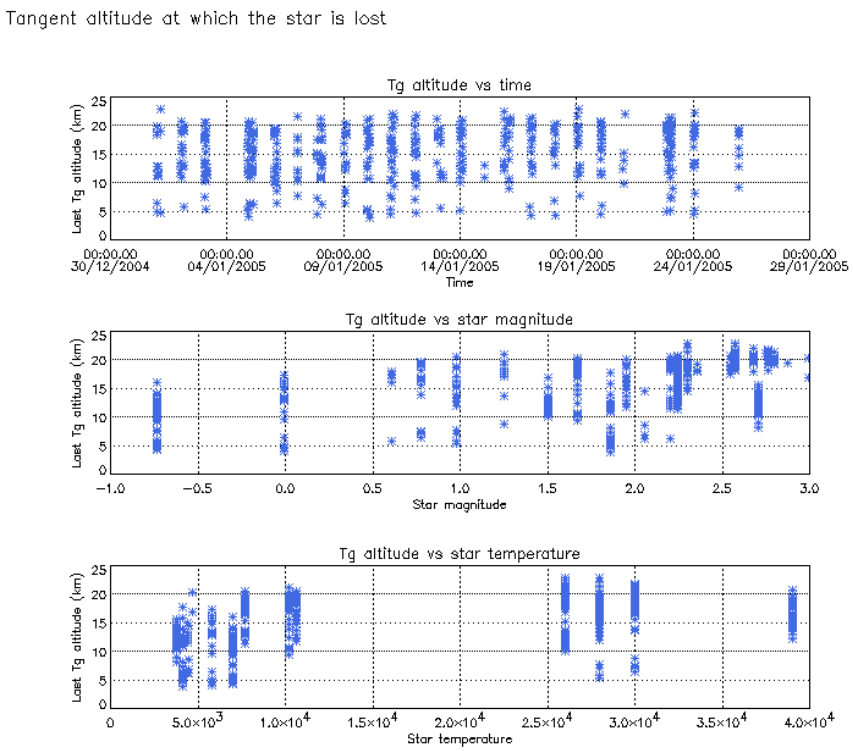

Figure 4.6-3: Last tangent altitude of the occultation (dark limb), point at which the star is lost

Tangent altitude at which the star is lost

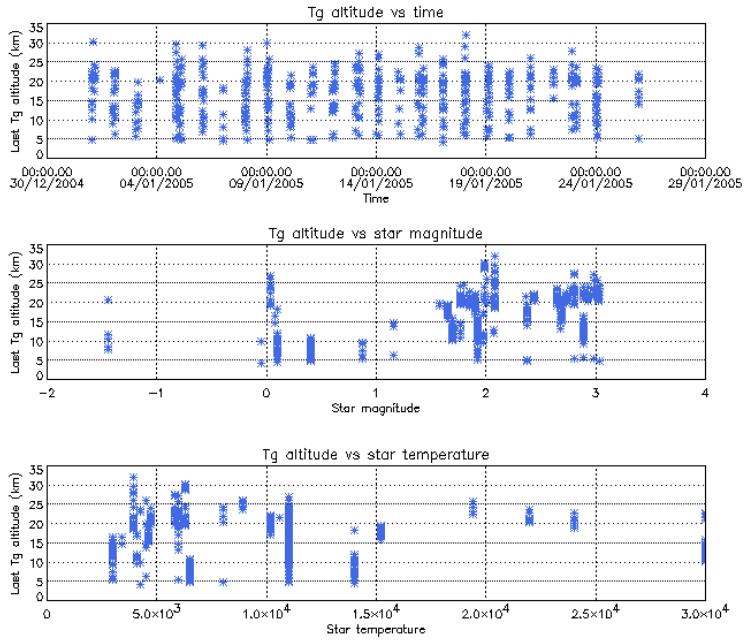

Figure 4.6-4: Last tangent altitude of the occultation (bright limb), point at which the star is lost

Tangent altitude at which the star is lost

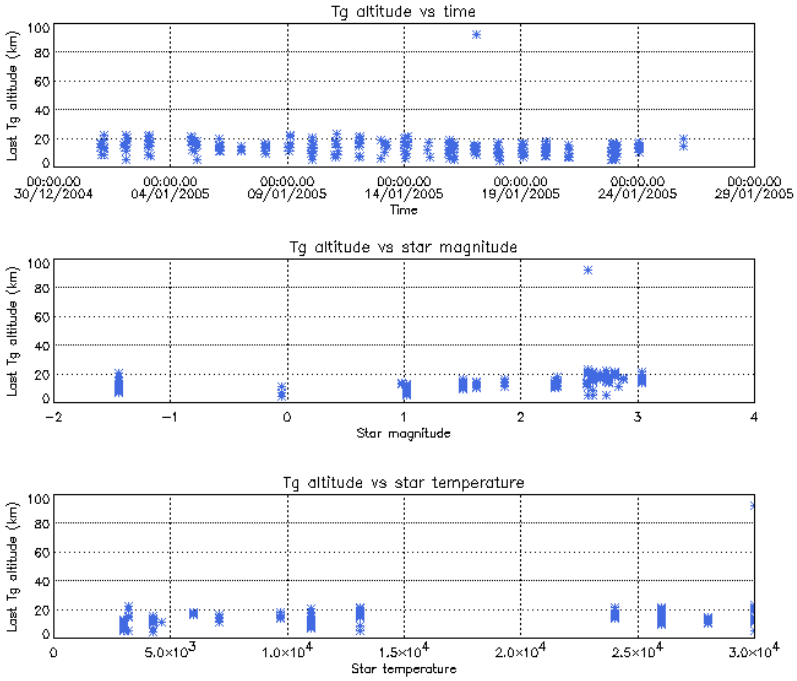

Figure 4.6-5: Last tangent altitude of the occultation (twilight limb), point at which the star is lost

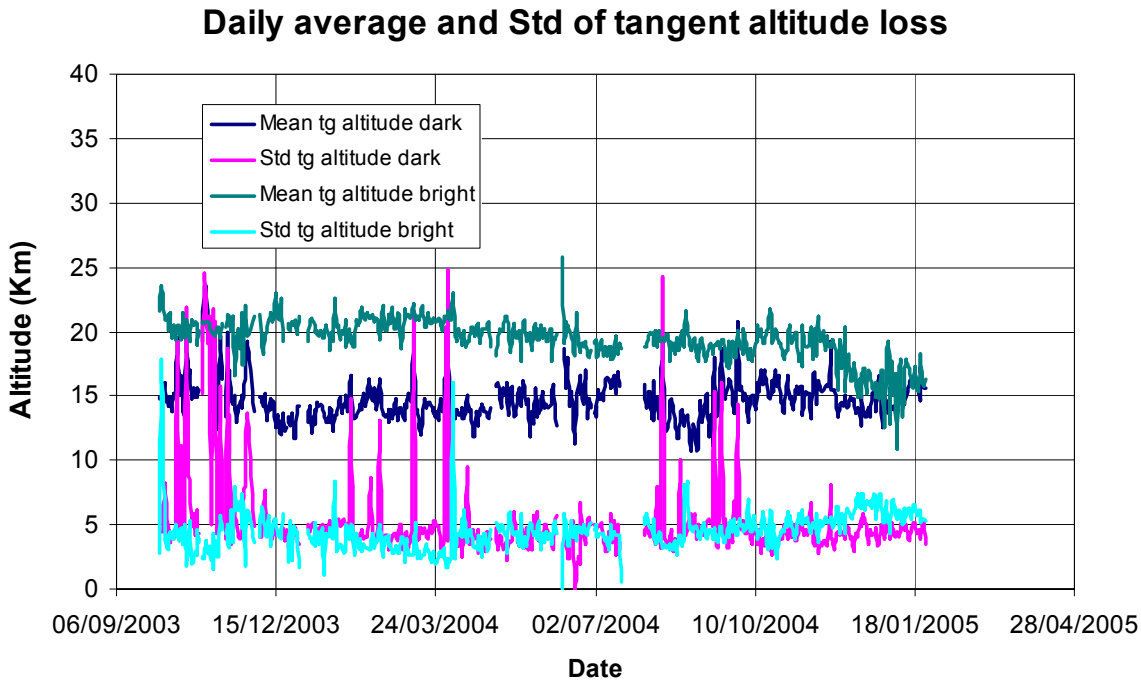

Figure 4.6-6: Daily average and STD of tangent altitude loss for the reporting period

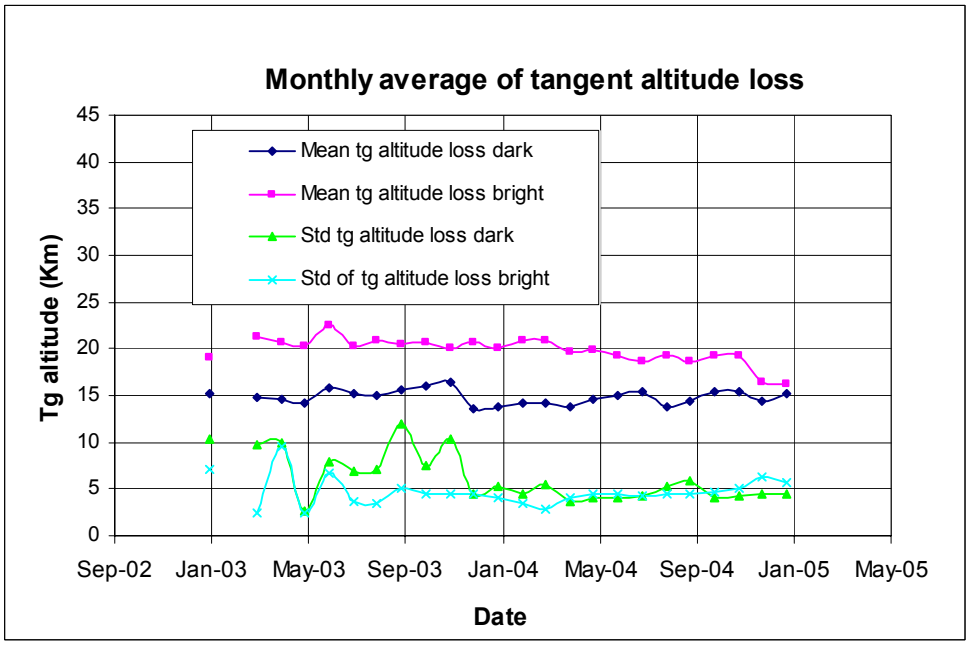

Figure 4.6-7: Monthly mean tangent altitude (and STD) at which the star is lost since January 2003

4.6.3 MOST ILLUMINATED PIXEL (MIP)

The MIP (Most Illuminated Pixel) is the star position on the SATU CCD in detection mode and it is recorded in the housekeeping data. The nominal centre of the SATU is pixel number **145** in elevation and number **205** in azimuth. The detection of the stars should not be far from this centre. All MIP values for one orbit every two days were extracted, averaged and plotted (fig. 4.6-8) until orbit 13472 (27th September 2004). After that orbit, and due to the importance of MIP data to monitor the ENVISAT pointing, every orbit is used to extract the MIP values. In order to be more accurate, only values of the MIP when GOMOS was in "DETECTION" pointing sub-mode are used.

As can be seen in fig. 4.6-8 the azimuth is always well within the threshold (table 4.6-1) since September 2002 even if a small variation is present. The elevation MIP has a significant variation (see the *note* below) till 12th December 2003 when a new PSO algorithm was activated in order to reduce the deviations of the ENVISAT platform attitude with respect to the nominal one. The annual amplitude of the MIP displacement is decreased from 18-20 pixels to 8-10 that means an important improvement of the ENVISAT pointing performance. This result confirms that, until now, the algorithm is working as expected. The MIP displacement will continue to be carefully monitored during the remaining mission.

Note: A MIP variation onto the SATU CCD of 50 pixels corresponds to a de-pointing of 0.1 degrees

Table 4.6-1: MIP Thresholds

MIP X	**Mean delta Az**	[198 - 210]
	Std delta Az	7
MIP Y	**Mean delta El**	[140 – 150]
	Std delta El	4

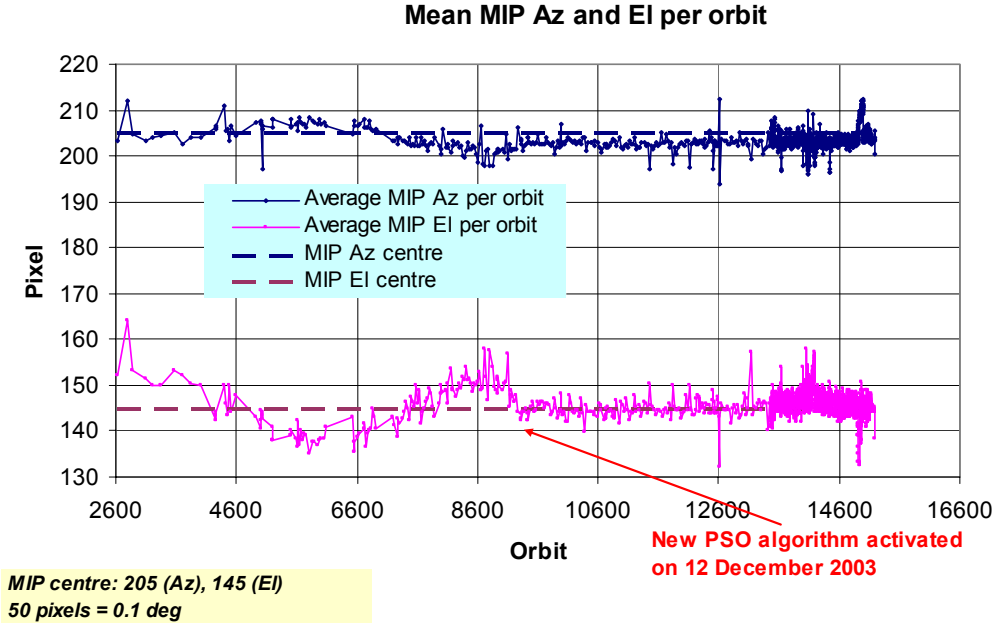

Figure 4.6-8: Mean values of MIP for some orbits since 1st September 2002 (see table 4.6-1)

Fig. 4.6-9 shows the standard deviation of azimuth and elevation that should be within the thresholds of table 4.6-1. Before orbit 13472 (all MIP values used for the average), the peaks mainly occur because data when no detection was performed, were also used for the average and STD calculation. The peaks observed after orbit 13472 mean that one (or more) star/s where detected very far from the SATU centre and, in this case, the star/s is lost during the centering phase (see section 3.2 for stars lost in centering).

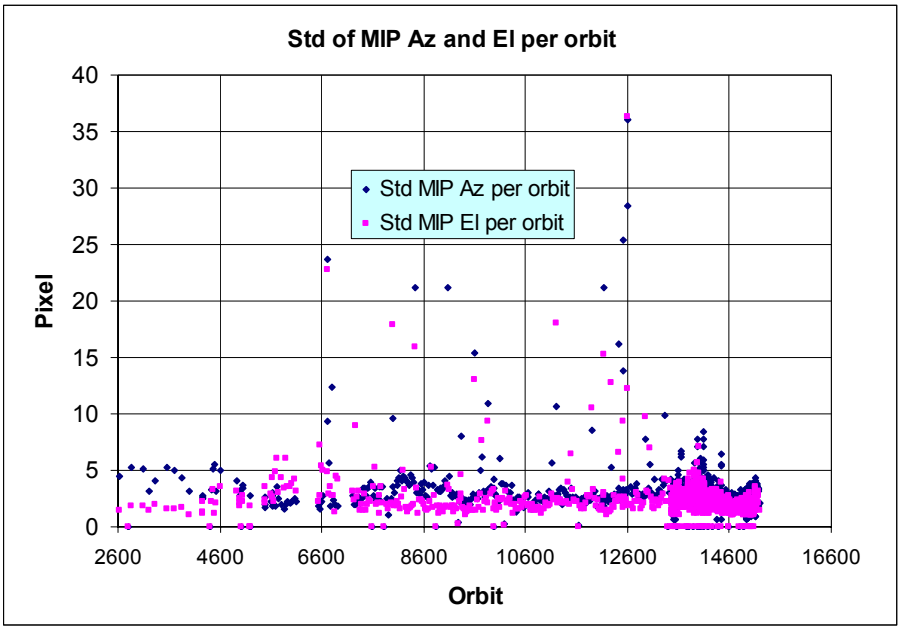

Figure 4.6-9: Standard deviation of MIP Azimuth and Elevation for some orbits since 1st September 2002 until end of reporting period (see table 4.6-1)

5 LEVEL 1 PRODUCT QUALITY MONITORING

About 10% of GOM_TRA_1P products have been received in the PCF for routine quality control and long term trend quality monitoring. The products with fatal errors (MPH error flag set) were around 1% of the products received during the reporting month and were not used for quality monitoring.

5.1 Processor Configuration

5.1.1 VERSION

The current level 1-processor software version for the operational ground segment is GOMOS/4.02 (see table 5.1-1). The product specification is PO-RS-MDA-GS2009_10_3H. This processor has been cleared for initial level 1 data release, with a disclaimer for known artefacts (http://envisat.esa.int/dataproducts/availability/disclaimers) that are currently being resolved and will be implemented in the next release (http://envisat.esa.int/dataproducts/availability).

ESA is also providing 2003 products that are reprocessed with the prototype processor GOPR 6.0a. See table 5.1-2 for prototype level 1b versions and modifications.

Table 5.1-1: PDS level 1b product version and main modifications implemented

Date	Version	Description of changes
23-MAR-2004	Level 1b version 4.02 at PDHS-E and PDHS-K	Algorithm baseline level 1b DPM 6.0 • Adding a new calibration parameters (these values are hard coded at the moment) • Removal of redundancy chain from code • Modifications in the processing to apply new configuration and calibration parameter • New algorithm to determine between dark, twilight and bright limb and to handle data accordingly • Added handling of source packages with invalid packet header • Added enumerations for all configuration flags • See ref. [2] for more details
31-MAY-2003	Level 1b version 4.00 at PDHS-E and PDHS-K	Algorithm baseline level 1b DPM 5.4: • Modulation correction step added after the cosmic rays detection processing • Inversion of the non-linearity and offset corrections • Modification of the computation of the estimated background signal measured by the photometers: use the spectrometer radiometric sensitivity curve and the photometer transfer function. • Use of the dark charge map at orbit level computed from the DSA (dark sky area) if any in the level 0 product • Implementation of a new unfolding algorithm for the photometer samples • See ref. [2] for more details
21-NOV-2002	Level 1b version 3.61 at PDHS-E and PDHS-K	Algorithm baseline DPM 5.3: • Review of some default values • New definition of one PCD flag (atmosphere) • Temporal interpolation of ECMWF data • See ref. [2] for more details

Table 5.1-2: GOPR level 1b product version and main modifications implemented

Date	Version	Description of changes
17-MAR-2004	GOPR 6.0a	• Provide SFA and SATU angles in degrees • Elevation angle dependency of the reflectivity LUT added in the algorithms • Ratio upper/star signal added (FLAGUC) • Add Dark Charge used for dark charge correction (per band) • Flag for illumination condition (PCDillum) • Minimum sample value for which the cosmic rays detection processing is applied (Crmin) is a function of gain index • Logic for computation of the flags attached to the reference star spectrum (Flref) modified • Add the computation of the sun direction in the inertial geocentric frame to be written in the level 1b and limb products. • Spectrometer effective sampling time added (To be completed)
25-JUL-2003	GOPR 5.4f	• The demodulation process is applied only in full dark limb and twilight limb conditions.

17-JUL-2003	GOPR 5.4e	• Sun zenith angle is computed in the geolocation process. The occultation is now classified into (0) full dark limb condition, (1) bright limb condition and (2) twilight limb condition. • No background correction applied in full dark limb condition. The location of the image of the star spectrum on the CCD array is no more aligned with the CCD lines.
02-JUL2003	GOPR 5.4d	• The maximum number of measurements is set to 509 (instead of 510) in the GOPR prototype.
17-MAR-2003	GOPR 5.4c	• Modification of the CAL ADFs (update of the limb radiometric LUT). The products are affected only if the limb spectra are converted into physical units • Modifications to allow compatibility with ACRI computational cluster (no modifications of the results) • Modification of the logic to handle dark charge map refresh at orbit level (DSA data is now directly processed by the level 1b processor if available in the level 0 product). No impact on the results
21-FEB-2003	GOPR 5.4b	• DC map values are rounded when written in the level 1b product • Modification of the CAL ADFs (update of the wavelength assignment of SPB1 and SPB2) • Modify the computation of flag_mod in the modulation correction routine
17-JAN-2003	GOPR 5.4a	• use the start and stop dates of the occultation when calling the CFI interpol instead of start and stop dates of the level 0 product • modify the ECMWF filename information in the SPH of the level 1b and limb products

5.1.2 AUXILIARY DATA FILES (ADF)

The ADF's files in tables 5.1-3, 5.1-4, 5.1-5, 5.1-6 and 5.1-7 have been disseminated to the PDS during the whole mission. For every type of file, the validity runs from the start validity time until the start validity time of the following one, but if an ADF file has been disseminated after the start validity time, it is obvious that it will be used by the PDHS-E and PDHS-K PDS only after the dissemination time (this happens the majority of the times). As the other ADF's, the calibration auxiliary file (GOM_CAL_AX) has been updated several times in the past (table 5.1-7) but the difference is that now it is updated in a weekly basis with only new DC maps, and that is why the files used in January are reported in a separate table (table 5.1-8) that will change from month to month. On 10th, 17th and 26th January new calibration ADF's were disseminated with updated DC maps of orbits 14966, 15066 and 15177 respectively (table 5.1-8). Note that the files outlined in yellow are the set of auxiliary files used during the reporting period.

Table 5.1-3: Table of historic GOM_PR1_AX files used by PDS for level 1b products generation

Used by PDS for Level 1b products generation in period	GOM_PR1_AX (GOMOS processing level 1b configuration file)
01-MAR-2002 → 29-MAR-2002	**GOM_PR1_AXVIEC20020121_165314_20020101_000000_20200101_000000** • Pre-launch configuration
30-MAR-2002 → 14-NOV-2002	**GOM_PR1_AXVIEC20020329_115921_20020324_200000_20100101_000000** • Changed num_grid_upper, thr_conv and max_iter in the atmospheric GADS
Not used	**GOM_PR1_AXVIEC20020729_083756_20020301_000000_20100101_000000** • Cosmic Ray mode + threshold • DC correction based on maps

	• Non-linearity correction disabled
Not used	**GOM_PR1_AXVIEC20021112_170331_20020301_000000_20100101_000000** • Central background estimation by linear interpolation + associated thresholds
15-NOV-2002 → 26-MAR-2003	**GOM_PR1_AXVIEC20021114_153119_20020324_000000_20100101_000000** • Same content as GOM_PR1_AXVIEC20021112_170331_20020301_000000_20100101_000000 but validity start updated so as to supersede according to the PDS file selection rules GOM_PR1_AXVIEC20020329_115921_20020324_200000_20100101_000000
27-MAR-2003 → 19-MAR-2004	**GOM_PR1_AXVIEC20030326_085805_20020324_200000_20100101_000000** • Same content as GOM_PR1_AXVIEC20021112_170331_20020301_000000_20100101_000000 but validity start updated so as to supersede according to the PDS file selection rules GOM_PR1_AXVIEC20020329_115921_20020324_200000_20100101_000000
20-MAR-2004 → 22-MAR-2004	**GOM_PR1_AXVIEC20040319_134932_20020324_200000_20100101_000000** • Ray tracing parameter changed: convergence criteria set to 0.1 microrad
23-MAR-2004 → 01-APR-2004 *Notes*: • This file was constructed from GOM_PR1_AXVIEC20030326_085805_20020324_200000_20100101_000000 (so without the ray tracing parameter changed) • This file was used by the GOMOS/4.02 processors before the IECF dissemination. The dissemination was done on 25th March 2004	**GOM_PR1_AXVIEC20040316_144850_20020324_200000_20100101_000000** GOM_PR1 ADF for version GOMOS/4.02, changes: • The central band estimation mode • Atmosphere thickness • Altitude discretisation
02-APR-2004	**GOM_PR1_AXVIEC20040401_083133_20020324_200000_20100101_000000** • Ray tracing parameter changed: convergence criteria set to 0.1 microrad

Table 5.1-4: Table of historic GOM_INS_AX files used by PDS for level 1b products generation

Used by PDS for Level 1b products generation in period	GOM_INS_AX (GOMOS instrument characteristics file)
01-MAR-2002 → 29-JUL-2002	**GOM_INS_AXVIEC20020121_165107_20020101_000000_20200101_000000** • Pre-launch configuration
30-JUL-2002 → 12-NOV-2002	**GOM_INS_AXVIEC20020729_083625_20020301_000000_20100101_000000** • Factors for the conversion of the SFA angles from SFM axes to GOMOS axes
13-NOV-2002 → 16-JUL-2003	**GOM_INS_AXVIEC20021112_170146_20020301_000000_20100101_000000** • No more invalid spectral range
Not used	**GOM_INS_AXVIEC20030716_080112_20030711_120000_20100101_000000** • New value for SFM elevation zero offset for redundant chain: 10004

17-JUL-2003	**GOM_INS_AXVIEC20030716_105425_20030716_120000_20100101_000000** • Bias induct azimuth redundant value set to -0.0084 rad (-0.4813 deg)

Table 5.1-5: Table of historic GOM_CAT_AX files used by PDS for level 1b products generation

Used by PDS for Level 1b products generation in period	GOM_CAT_AX (GOMOS Stat Catalogue file)
01-MAR-2002	**GOM_CAT_AXVIEC20020121_161009_20020101_000000_20200101_000000** • Pre-launch configuration

Table 5.1-6: Table of historic GOM_STS_AX files used by PDS for level 1b products generation

Used by PDS for Level 1b products generation in period	GOM_STS_AX (GOMOS Star Spectra file)
01-MAR-2002	**GOM_STS_AXVIEC20020121_165822_20020101_000000_20200101_000000** • Pre-launch configuration

Table 5.1-7: Table of historic GOM_CAL_AX files used by PDS for level 1b products generation

Used by PDS for Level 1b products generation in period	GOM_CAL_AX (GOMOS Calibration file)
01-MAR-2002 → 29-JUL-2002	**GOM_CAL_AXVIEC20020121_164808_20020101_000000_20200101_000000** • Pre-launch configuration
Not used	**GOM_CAL_AXVIEC20020121_142519_20020101_000000_20200101_000000** • Pre-launch configuration
30-JUL-2002 → 12-NOV-2002	**GOM_CAL_AXVIEC20020729_082426_20020717_193500_20100101_000000** • Band setting information • Wavelength assignment • Spectral dispersion LUT • ADC offset for Spectrometers • PRNU maps • Thermistor coding LUT • DC maps
Not used	**GOM_CAL_AXVIEC20021112_165603_20020914_000000_20100101_000000** • Band setting information • DC maps • PRNU maps • Wavelength assignment • Spectral dispersion LUT • Radiometric sensitivity LUT (star and limb) • SP-FP intercalibration LUT • Vignetting LUT • Reflectivity LUT • ADC offset
13-NOV-2002 → 30-JAN-2003	**GOM_CAL_AXVIEC20021112_165948_20021019_000000_20100101_000000** • Only DC maps updated
31-JAN-2003 → 11-APR-2003	**GOM_CAL_AXVIEC20030130_133032_20030101_000000_20100101_000000**

	• Only DC maps updated (using DSA of orbit 04541)
12-APR-2003 → 02-JUN-2003	**GOM_CAL_AXVIEC20030411_065739_20030407_000000_20100101_000000** • Modification of the radiometric sensitivity curve for the limb spectra. Note that the modification of this LUT has no impact on the GOMOS processing. The LUT is just copied into the level 1b limb product for user conversion purpose. • Updated DC map only (using DSA of orbit 05762).
03-JUN-2003: from this date onwards, mainly updates to DC maps are done. Every month, the table of new GOM_CAL files with **only** DC maps updated is provided (table 5.1-8). Eventual changes to this file not corresponding only to DC maps updates will be reported in this table.	**GOM_CAL_AXVIEC20030602_094748_20030531_000000_20100101_000000** • Updated DC maps only (using DSA of orbit 06530)
13-FEB-2004 → 23-FEB-2004	**GOM_CAL_AXVIEC20040212_103916_20040209_000000_20100101_000000** • Update of the reflectivity LUT • Updated DC maps (Orbit 10194, date 11-FEB-2004)

Table 5.1-8: Calibration ADF for reporting period. These files are updated (only with DC maps) in a 8-10 days basis

Used by PDS for Level 1b products generation in period	GOM_CAL_AX (GOMOS Calibration file)
18-DEC- 2004 → 10-JAN-2005	**GOM_CAL_AXVIEC20041217_142407_20041216_000000_20100101_000000** (orbit 14622, date 16 DEC 2004)
11-JAN-2005 → 17-JAN-2005	**GOM_CAL_AXVIEC20050110_095700_20050108_000000_20100101_000000** (orbit 14966, date 09 JAN 2005)
18-JAN-2005 → 26-JAN-2005	**GOM_CAL_AXVIEC20050117_132951_20050115_000000_20100101_000000** (orbit 15066, date 16 JAN 2005)
27-JAN-2005	**GOM_CAL_AXVIEC20050126_111922_20050123_000000_20100101_000000** (orbit 15177, date 24 JAN 2005)

5.2 Quality Flags Monitoring

In this section it is monitored some Product Quality information stored in level 1b products that did not have a fatal error (MPH error flag not set).

On the one hand, for every product we have information of the **number of measurements** where a given problem was detected (i.e. number of invalid measurements, number of measurements containing saturated samples, number of measurements with demodulation flag set…). On the other hand, there are **flags** that indicate problems within the product (i.e. flag set to one if the reference spectrum was computed from the database, flag set to zero if SATU data were not used…).

For the information on the number of measurements a plot of percentages with respect to time is provided in fig. 5.2-1. Part of this information, the most relevant one, is also plotted in a world map as a function of ENVISAT position: % of cosmic ray hits per profile, % of datation errors per profile, % of star falling outside the central band per profile and % of saturation errors per profile (fig.5-2.2).

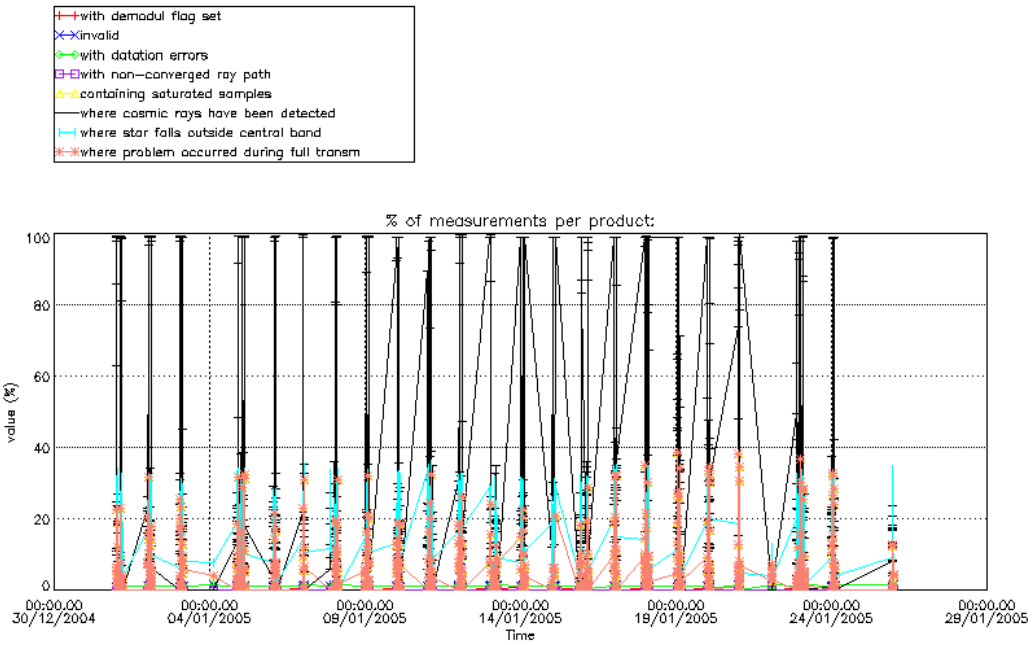

Figure 5.2-1: Level 1b product quality monitoring with respect to time

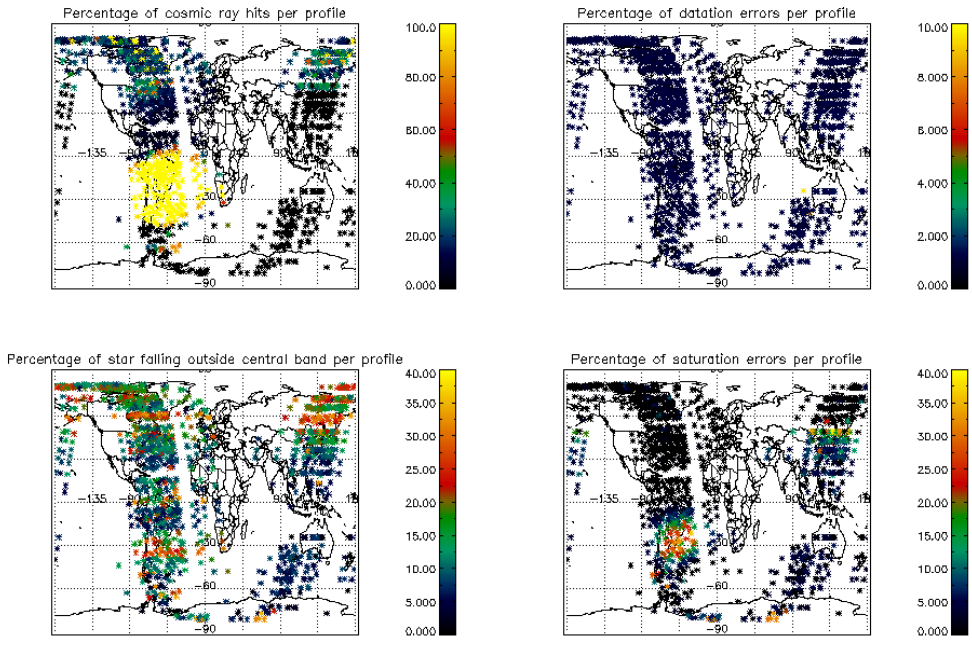

Figure 5.2-2: Level 1b product quality monitoring with respect to geolocation of ENVISAT

It can be seen from fig. 5.2-1 that the cosmic rays hits occurred several times for the 95% of the measurements of the products. Looking at fig. 5.2-2 it can be clearly observed that this high percentage

occurred when the satellite crossed the South Atlantic Anomaly (SAA) zone. High percentage of cosmic rays has been detected also over the poles (on dates 17 and 20 January) due to the eruption of the sunspot 720. Also the percentage of saturation errors per profile increased over SAA zone. Another observation from fig. 5.2-1 is that, for many products, the 25 % of the measurements have the star signal falling outside the central band. In fig. 5.2-2 it is observed that this percentage occurred mainly during the ascending part of the orbit (night-side of the orbit) while in the descending part (day-side of the orbit) the percentage is less than 10 %. This is because during the night the stars are lost deeper within the atmosphere and the turbulence phenomena become more important, producing the star to be less 'focused' on the spectrometers central band. The other values (% of invalid measurements per product, % of measurements per product with datation errors…) are quite low.

The flag information is given in table 5.2-1. It is reported also the percentage of the products that have at least one measurement with demodulation flag set.

Table 5.2-1: Percentage of products during the reporting period with:

At least one measurement with demodulation flag set:	22.1731 %
Reference spectrum computed from DB:	0.00000 %
Reference spectrum with small number of measurements:	0.00000 %
SATU data not used:	0.00000 %

5.2.1 QUALITY FLAGS MONITORING (EXTRACTED FROM LEVEL 2 PRODUCTS)

In this section it is plotted the Product Quality information coming from the level 1 processing but stored also in the level 2 products. Only products that did not have a fatal error (MPH error flag not set) are considered. The purpose of using the level 2 data is simply that the percentage of level 2 products arriving in PCF for the quality monitoring is much higher. For the reporting month, 77% of the archived products have been received. The plots are very similar to fig. 5.2-1 and 5.2-2 (demodulation flag information is not included) but separating ascending from descending passes. The ascending part of the orbit (above -70^{o} latitude) is in dark limb while the descending (below 58 ^{o} latitude) is in bright limb.

Fig. 5.2-3 and 5.2-4 present some quality information as a function of the time whereas in fig. 5.2-5 and 5.2-6 the plot is respect to the satellite position at the beginning of the occultations. In ascending (fig. 5.2-5) the SAA is perfectly localized by the high percentage of cosmic ray hits per product (upper left panel). Also the high solar activity can be observed with a high percentage of cosmic rays detected over the poles. It is not the same if we look fig. 5.2-6, because in descending below 58 ^{o} latitude, the occultations are in bright limb conditions and the cosmic rays detection processing is not activated.

Another clear difference between ascending and descending is that in ascending (fig. 5.2-3) the percentage of measurements "where a problem occurred during the full transmission" per product is around 2% while for the descending passes is around 10%. This is due to the saturation that occurs mainly in bright limb. In ascending the saturation occurs over the SAA zone but it is quite low elsewhere.

There are some products with a high percentage of invalid measurements and measurements with datation errors (fig. 5.2-4). These products are mainly partial occultations: the last occultation of a level 0

product; being the entire occultation included in the following level 0 file. These products have a degraded quality and should not be used by the users.

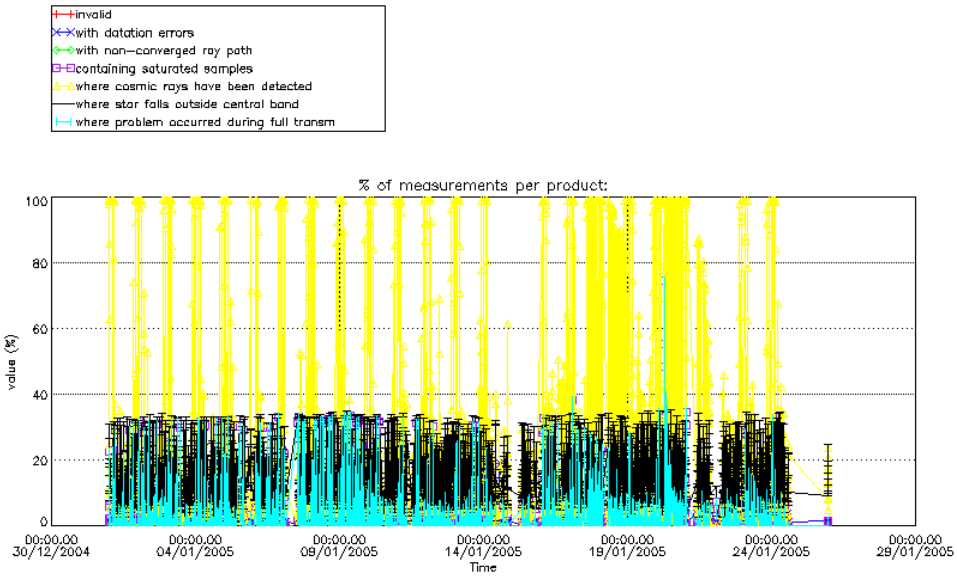

Figure 5.2-3: Level 1b product quality monitoring with respect to time <u>ASCENDING</u> ENVISAT passes

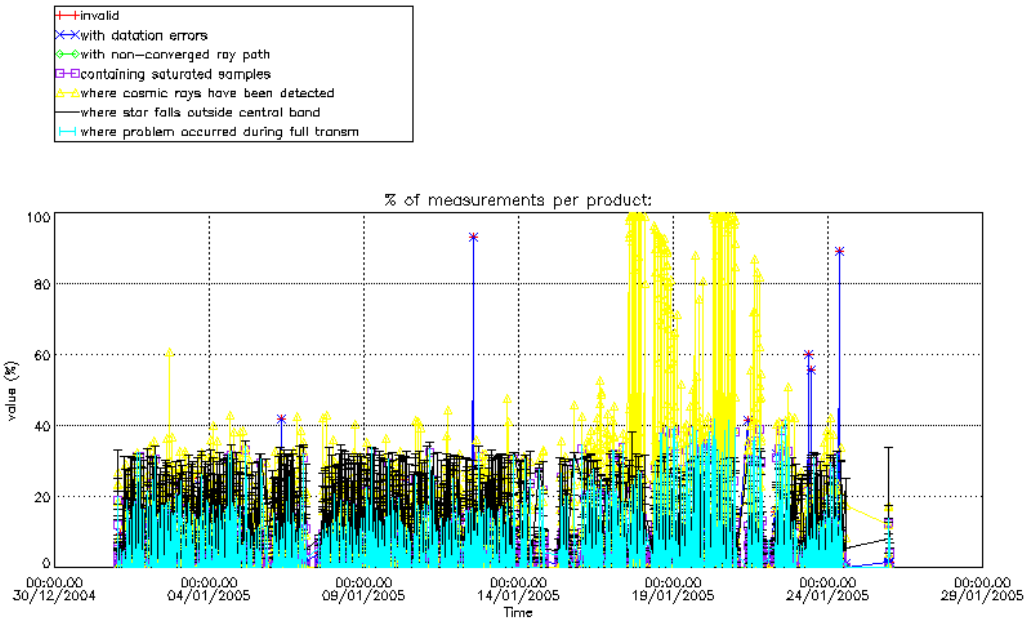

Figure 5.2-4: Level 1b product quality monitoring with respect to time <u>DESCENDING</u> ENVISAT passes

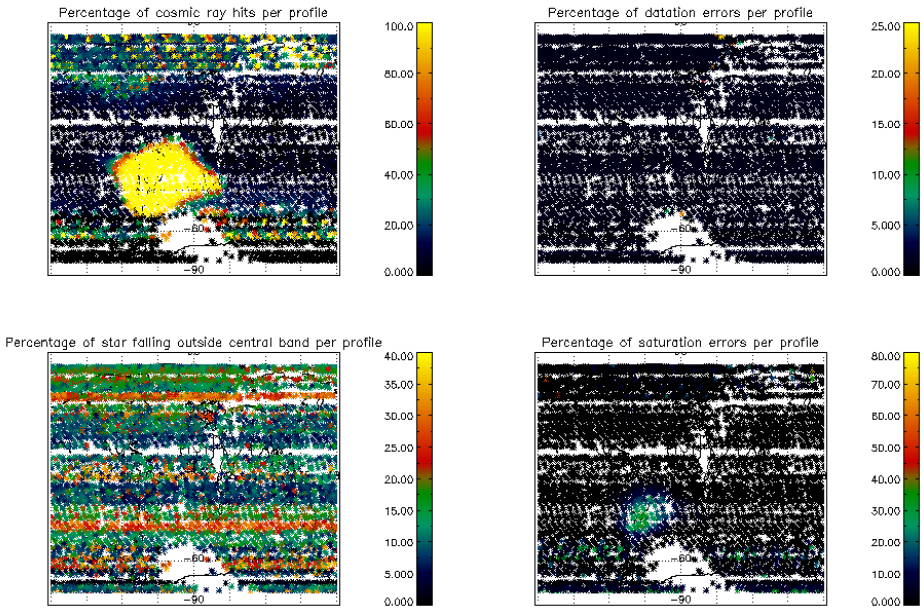

Figure 5.2-5: Level 1b product quality monitoring with respect to geolocation for ASCENDING ENVISAT passes

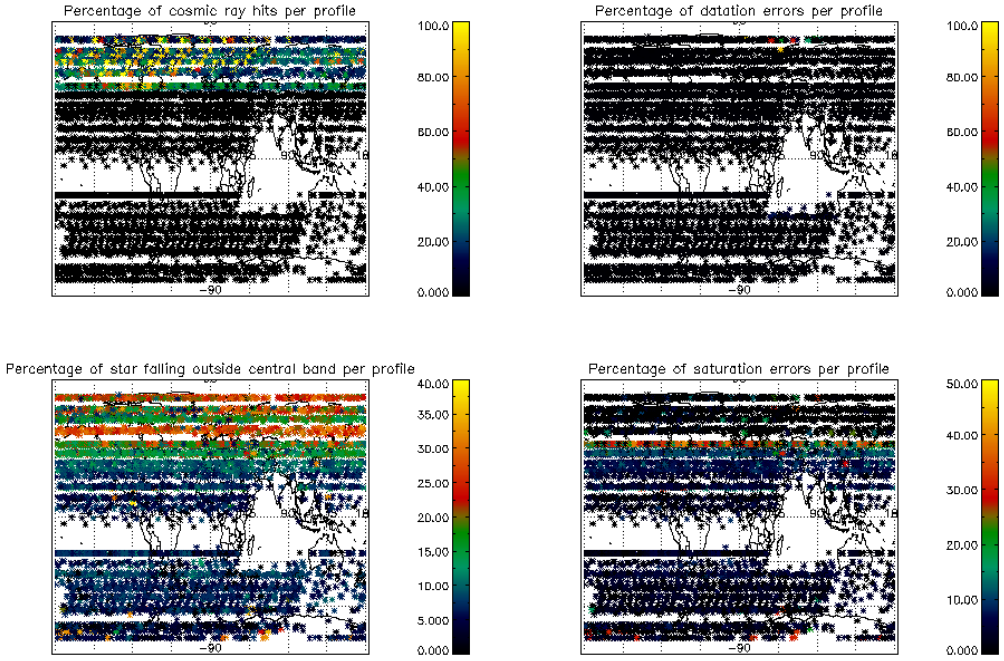

Figure 5.2-6: Level 1b product quality monitoring with respect to geolocation for DESCENDING ENVISAT passes

5.3 Spectral Performance

No new spectral calibration has been performed during the reporting period. Last calibration exercises have shown that warning values have been reached.

The values reported (table 5.3-1) are, for every star ID (1, 2, 4, 9, 18, 25), the wavelength of the first useful pixel of SPA2. This value is calculated by addition to the actual wavelength assignment, the spectral shift for which a maximum correlation has been found between the reference spectrum and the one of the occultation. During the last wavelength calibration analysis performed using two occultations, the spectral shifts were -0.098 for star id number 2 and -0.1 for star id number 1 (see table 5.3-1). These shifts are greater than 0.07 (warning value) and QWG investigations that have been initiated already in March 2004 will continue.

The star number 4 is left in table 5.3-1 even if the values of the wavelength are very different from the nominal one. It should be just kept in mind that the values of the shift should be always of the same order (~0.4) but this star will not be used for calibration purposes.

Table 5.3-1: Wavelength assignment calculated for several occultations since November 2002

Star ID / Level 0 date	1	2	4	9	18	25
20021112_062935	Occ.30: 690.455750	Occ.26: 690.458740		Occ.28: 690.492981		
20021219_102754		Occ.33: 690.468140	Occ.26: 690.875122			
20030101_151630	Occ.3: 690.445068	Occ.37: 690.466003	Occ.30: 690.878540			
20030110_121504		Occ.32: 690.465088	Occ.25: 690.882385			
20030201_090221						Occ.21: 690.492981
20030415_123156			Occ.29: 690.959534		Occ.20: 690.552002	Occ.28: 690.492981
20030419_170041			Occ.29: 690.957520		Occ.23: 690.555420	
20030428_072600					Occ.19: 690.553645	Occ.28: 690. 492981
20030717_053233				Occ. 22: 690.473816	Occ. 26: 690.446594	
20040123_091615	Occ.1: 690.400513 Occ.40: 690.401550	Occ.35: 690.415161	Occ.27: 690.852478			
20040222_065917			Occ.25: 690. 850830			Occ.21: 690. 492981
20040128_163559	Occ.3: 690.399414					Occ.23: 690. 492981
20040804_123934	Occ.20 690.411377	Occ.24 690.404724		Occ.25 690.397522	Occ.29 690.397156	
20041101_074131	Occ. 26 690.403748	Occ. 21 690.392700		Occ. 24 690.398254		
20050101_014125	Occ.18 690.386841	Occ.14 690.394348	Occ. 6: 690.811157			

5.4 Radiometric Performance

5.4.1 RADIOMETRIC SENSITIVITY

The monitoring performed consists in the calculation of the radiometric sensitivity of each CCD by computing the ratio between parts of the reference spectrum using specific stars. The parts of spectrum used are:

- UV: 250–300 nm
- Yellow: 500–550 nm
- Red: 640–690 nm
- Ir1: 761-770 nm
- Ir2: 935-944 nm

For the spectrometers the ratios are with respect to the 'yellow' spectral range. For the photometers, the ratio is calculated dividing the mean photometer signal above the atmosphere (115 km) by the 'yellow' spectral range (for PH1) or by the 'red' spectral range (for PH2).

The variation of the ratio should be within a given threshold actually set to 10% (see table 5.4-1 that corresponds to fig. 5.4-1). For every star, this variation is calculated as the difference between the maximum (or minimum) ratio, and the mean over the 15 first values (if there are not 15 values computed yet, all values are used).

Table 5.4-1: Variation of RS for the different ratios (corresponds to fig. 5.4-1). Should be less than 10%

Star Id	% Variation of UV ratio	% Variation of Red ratio	% Variation of IR1 ratio	% Variation of IR2 ratio	% Variation of Ph1 ratio	% Variation of Ph2 ratio
1	2.04276	0.511867	0.401701	0.250543	30.8640	70.2278
2	0.416756	0.652793	0.625175	0.383392	8.27717	7.93166
4	0.150048	0.838286	1.52463	1.30163	8.08780	23.5227
9	4.63446	0.416139	0.783493	0.466555	835.855	2624.41
18	0.990748	0.681692	0.844914	0.852089	1865.10	5139.44
25	14.3013	0.699922	0.654513	1.12662	28.0870	147.396

Values outside the warning threshold set to 10% are observed mainly for the photometers, and investigations were performed by the QWG. An inaccurate reflectivity correction LUT was suspected to be the cause of the increase but a new one is in use since 12th February 2004 and the results did not change.

In fig. 5.4-2 the two fast photometer ratios have been splinted by stars, so one plot per star is presented. As it can be seen, for star id 9 only two points are the cause of the big variation of the percentage while for star id 18 it is just one point. If we plot the ratios for star 9 and 18 without taking into account the peaks (fig. 5.4-3), it can be seen that the ratios for the first one are stable while for the second, a variation is detected. This variation, visible also for star 25, depends the period of the year and should be linked to the star itself and not to any photometers sensitivity problem.

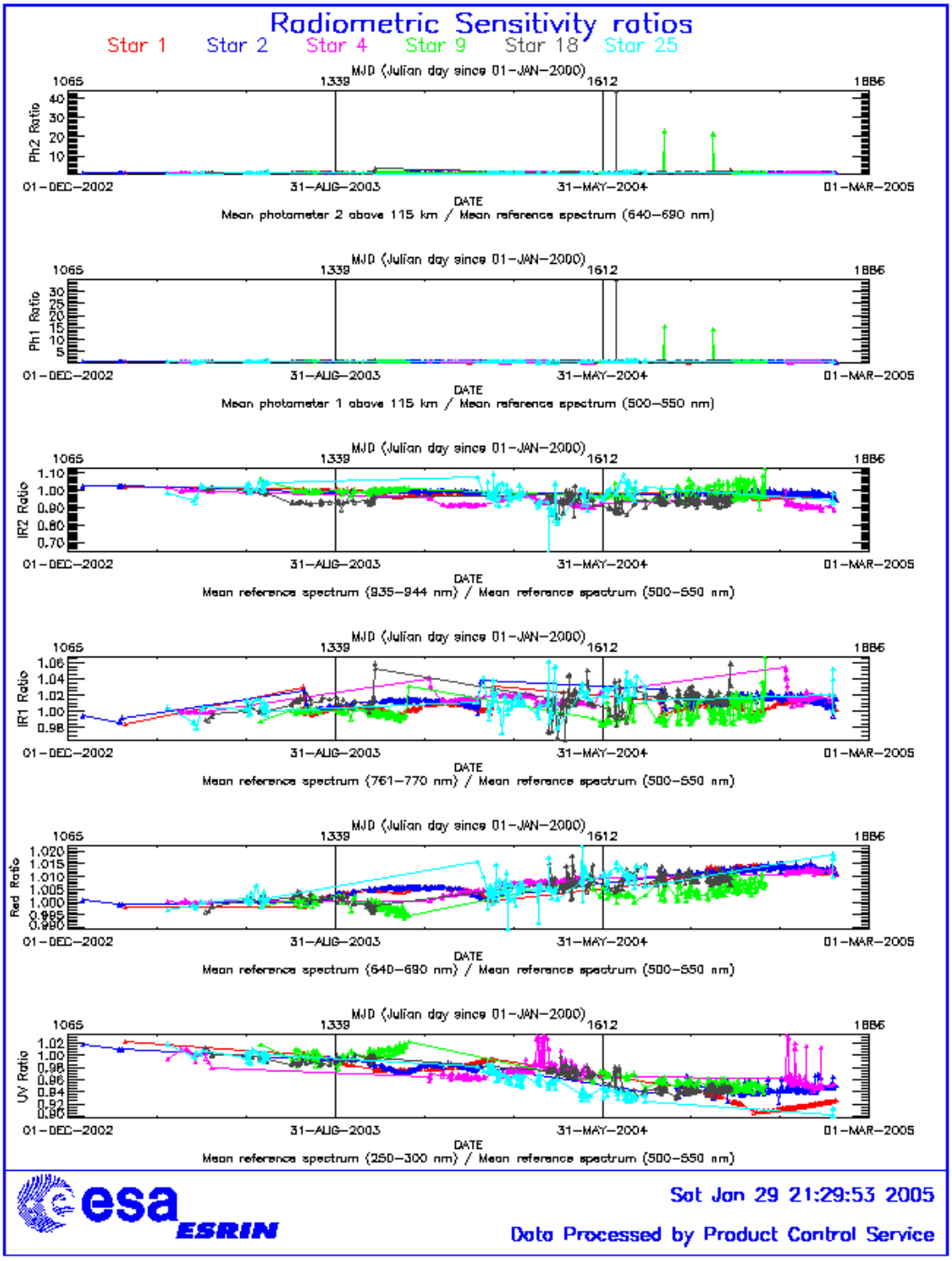

Figure 5.4-1: Radiometric sensitivity ratios since December 2002

For star 25 also the UV ratio is greater than 10%. Looking at the fig. 5.4-1, it is clear that there is a global decrease of UV ratios for all the stars. This confirms the expected degradation suffered by the UV optics that is, anyway, very small considering also the small variation for the rest of the stars (table 5.4-1).

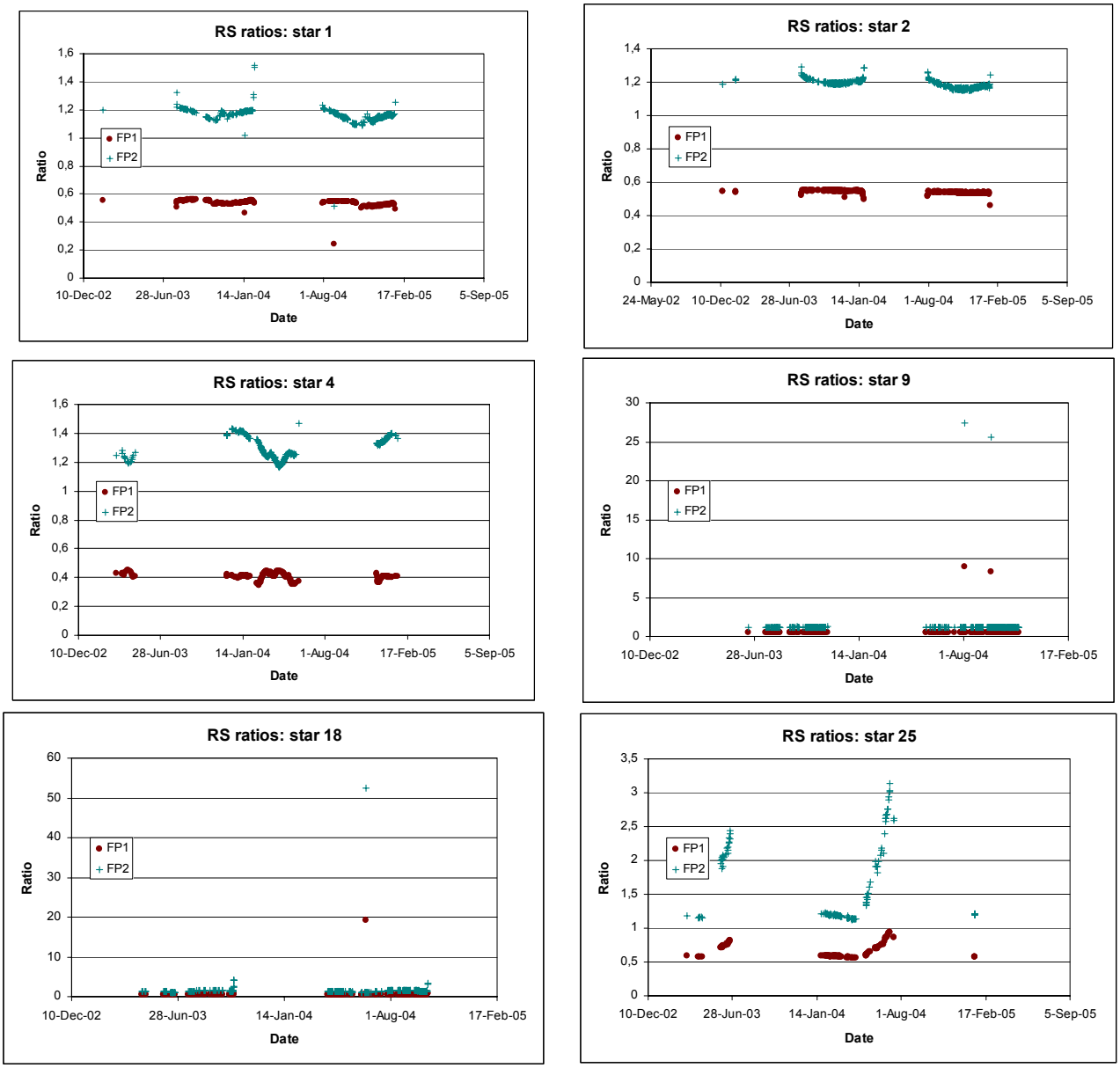

Figure 5.4-2: Fast Photometer ratios for the different monitoring stars. They are the same ratios plotted in fig. 5.4-1 (the ones corresponding to PH1 and PH2) but now one plot per star

The products with photometer signal that caused the high peaks on star 9 and 18 have been studied in depth. These products have few missing (empty) records at the beginning of the occultation but the reference spectra have been computed successfully and the products are considered to be with nominal quality.

In fig. 5.4-4 the photometers signal has been compared to nominal photometer signals of the same stars and, as it can be seen, the signals are very high with respect to nominal photometer signals. Apparently, the missing packets at the beginning of the occultations have created a problem in the photometer unfolding algorithm. Investigations are ongoing at this time to find this suspected bug.

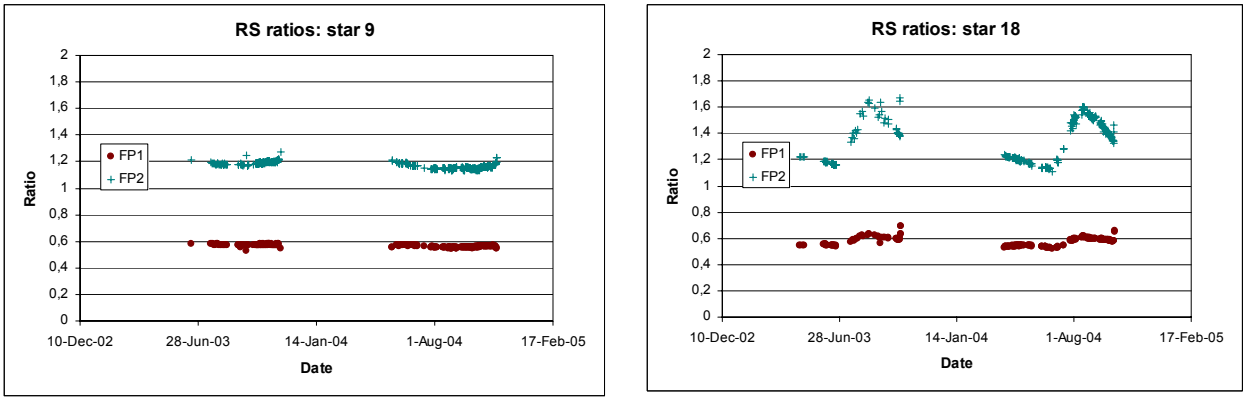

Figure 5.4-3: Fast Photometer ratios for stars 9 (left) and 18 (right) without taking into account the peaks

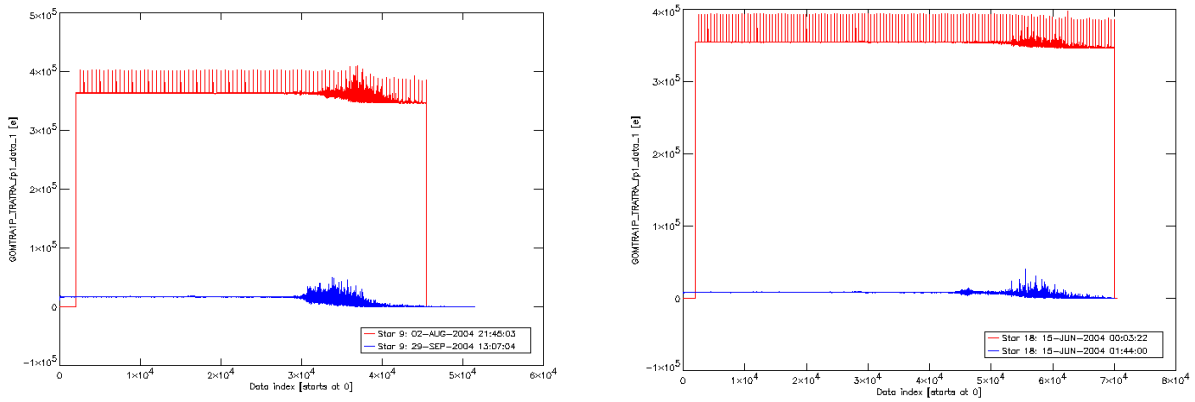

Figure 5.4-4: Photometer signals for star 9 (left) and star 18 (right). The red signals are the ones causing the big peaks on the radiometric sensitivity ratios. The blue signal is a typical photometer signal for the same stars

5.4.2 PIXEL RESPONSE NON UNIFORMITY

No new PRNU calibration has been performed during the reporting period. This means that the PRNU maps inside the ADF remain as they are without any change for the moment.

5.5 Other Calibration Results

Future reports will address other calibration results, when available.

6 LEVEL 2 PRODUCT QUALITY MONITORING

Level 2 products from the operational ground segment have been disseminated during January to the users. About 77% of GOM_NL__2P products have been received in the PCF for routine quality control and long term trend monitoring. The products with fatal errors (MPH error flag set) were around 0.7% of the products received during the reporting month and were not used for quality monitoring.

6.1 Processor Configuration

6.1.1 VERSION

The current level 2-processor software version for the operational ground segment is GOMOS/4.02 (see table 6.1-1). The product specification is PO-RS-MDA-GS2009_10_3H. The improvements defined at the first Validation Workshop have been implemented into the prototype processor GOPR 6.0a (see table 6.1-2), before implementation into the operational one. In the mean time, Cal/Val teams are supplied with selected data sets generated by this prototype processor (version also used for the GOMOS reprocessing (see section 6.1.3).

Table 6.1-1: PDS level 2 product version and main modifications implemented

Date	Version	Description of changes
23-MAR-2003	Level 2 version 4.02 at PDHS-E and PDHS-K	Algorithm baseline level 2 DPM 5.5: Section 3 • Add references to technical notes on Tikhonov regularization • Change High level breakdown of modules: SMO/PFG • Change parameter: NFS in l2 ADF • Change parameter σ_G in l2 ADF (Table 3.4.1.1-II) • Change content of Level 2/res products - GAP • Change time sampling discretisation • Add covariance matrix explanation Section 5 • Replace SMO by PFG VER-1/2: Depending on NFS, Apply either a Gaussian filter or a Tikhonov regularization to the vertical inversion matrix • Unit conversion applied on kernel matrix • Suppress VER-3 Section 6 • GOMOS Atmospheric Profile (GAP): not used in this version • Time sampling in equation (6.5.3.7-73) • See ref. [3] for more details

31-MAY-2003	Level 2 version 4.00 at PDHS-E and PDHS-K	Algorithm baseline level 2 DPM 5.4: • Revision of some default values • Add a new parameter • Transmission model computation: suppress tests on valid pixels and species • Apply a Gaussian filter to the vertical inversion matrix • Very low signal values are substituted by threshold value • See ref. [3] for more details
21-NOV-2002	Level 2 version 3.61 at PDHS-E and PDHS-K	Algorithm baseline level 2 DPM 5.3a: • Revision of some default values • Wording of test T11 • Dilution term computation of jend • Covariance computation scaling applied before and after • See ref. [3] for more details

Table 6.1-2: GOPR level 2 product version and main modifications implemented

Date	Version	Description of changes
17-MAR-2004	GOPR 6.0a	• Rename Turbulence MDS into High Resolution Temperature MDS (HRTP) • Add vertical resolution per species in local densities MDS • Add Solar zenith angle at tangent point and at satellite level in geolocation ADS • Add "tangent point density from external model" in geolocation ADS • Suppress contribution of "tangent point density from external model" in "local air density from GOMOS atmospheric profile" in geolocation ADS (to be completed)
18-AUG-2003	GOPR 5.4d	• Tikhonov regularisation is implemented
18-MAR-2003	GOPR 5.4b	• Modification to implement the computation of Tmodel for spectrometer B (in version 5.4b, the Tmodel for SPB is still set to 1)
30-JAN-2003	GOPR 5.4a	• Modifications for ACRI internal use only. No impact on level 2 products.

6.1.2 AUXILIARY DATA FILES (ADF)

The ADF's files in table 6.1-3 and 6.1-4 are used by the PDS to process the data from level 1 to level 2. For every type of file, the validity runs from the start validity time until the start validity time of the following one, but if an ADF file has been disseminated after the start validity time, it is obvious that it will be used by the PDHS-E and PDHS-K PDS only after the dissemination time (this happens the majority of the times).

Table 6.1-3: Table of historic GOM_PR2_AX files used by PDS for level 2 products generation

Used by PDS for Level 2 products generation in period	GOM_PR2_AX (GOMOS Processing level 2 configuration file)
01-MAR-2002 → 29-JUL-2002	**GOM_PR2_AXVIEC20020121_165624_20020101_000000_20200101_000000** • Pre-launch configuration
30-JUL-2002 → 02-SEP-2002	**GOM_PR2_AXVIEC20020729_083851_20020301_000000_20100101_000000** • Maximum value of chi2 before a warning flag is raised (set to 5) • Maximum number of iterations for the main loop (set to 1)
03-SEP-2002 → 12-NOV-2003	**GOM_PR2_AXVIEC20020902_151029_20020301_000000_20100101_000000** • Maximum value of chi2 before a warning flag is raised (set to 100)
13-NOV-2003 → 22-MAR-2004	**GOM_PR2_AXVIEC20021112_170458_20020301_000000_20100101_000000** • Smoothing mode • Hanning filter • Number of iterations • Spectral windows to suppress the O2 absorption in the high spectral range of SPA2
23-MAR-2004 *Note*: this file was used by the GOMOS/4.02 processors before the IECF dissemination. The dissemination was done on 25th March 2004	**GOM_PR2_AXVIEC20040316_145613_20020301_000000_20100101_000000** • Pressure at the top of the atmosphere • Number of GOMOS sources data (used in GAP) • Activation flag for GOMOS sources data (GAP) • Smoothing mode (after the spectral inversion) • Atmosphere thickness

Table 6.1-4: Table of historic GOM_CRS_AX files used by PDS for level 2 products generation

Used by PDS for Level 2 products generation in period	GOM_CRS_AX (GOMOS Cross Sections file)
01-MAR-2002 → 08-MAR-2002	**GOM_CRS_AXVIEC20020121_164026_20020101_000000_20200101_000000** • Pre-launch configuration
09-MAR-2003 → 29-JUL-2002	**GOM_CRS_AXVIEC20020308_185417_20020101_000000_20200101_000000** • Corrected NUM_DSD in MPH - was 14 and is now 19 - and corrected spare DSD format by replacing last spare by carriage returns in file GOM_CRS_AXVIEC20020121_164026_20020101_000000_20200101_000000
30-JUL-2002 → 25-MAR-2004	**GOM_CRS_AXVIEC20020729_082931_20020301_000000_20100101_000000** • O3 cross-sections summary description (SPA) • NO3 cross-sections summary description • O2 transmissions summary description • H2O transmissions summary description • O3 cross sections (SPA)
26-MAR-2004 *Note*: the file was disseminated on 27 Jan 2004 but could not be used by PDS until version GOMOS/4.02 was in operation	**GOM_CRS_AXVIEC20040127_150241_20020301_000000_20100101_000000** • Update of the O2 and H2O transmissions (S.A input) • Extension by continuity of the O3 cross-section for SPB

6.1.3 RE-PROCESSING STATUS

To provide Cal/Val teams with early access to improved algorithms, selected occultations are processed with the prototype processor and made available to ACVT members. In addition, reprocessing of the full 2003 historic dataset has been performed with the prototype processor, and activities to complete the historic archive with the complete 2002 and 2004 dataset are underway. Data can be retrieved via web query from http://www.enviport.org/gomos/index.jsp. FTP access to bulk reprocessing results (one tar file of GOMOS products per day) is allowed from the D-PAC: ftp://gomo2usr@ftp-ops.de.envisat.esa.int.

The table 6.1-5 presents the status of the GOMOS reprocessing task in terms of availability of the instrument, level 0 input products and level 1b/2 output products. The status is presented by cycle. Each cycle is made of 501 orbits or 35 days. The last three columns of the table indicate the percentage of availability of each item with respect to the instrument availability in observation mode (i.e. for example without taking account the calibration or DSA observation of GOMOS).Values greater than 100% may occur due to the fact that some calibration observations are not taken into account in the instrument availability but they can be processed. See more details on http://www.fr-acri.com/gomval_web/news/board.htm

Table 6.1-5: Summary of reprocessing status at ACRI

Cycle	Orbits	Cycle Time Interval	% Instr. Availability	% L0 in ACRI	% Lv1b/L2 in ACRI
5	556-1056	08/04/02 21:59 - 13/05/02 20:18	89.6	0.0	0.0
6	1057-1557	13/05/02 21:59 -17/06/02 20:18	86.4	0.0	0.0
7	1558-2058	17/06/02 21:59 - 22/07/02 20:18	88.8	0.2	0.0
8	2059-2559	22/07/02 21:59 - 26/08/02 20:18	88.0	0.0	0.0
9	2560-3060	26/08/02 21:59 - 30/09/02 20:18	75.0	7.2	0.0
10	3061-3561	30/09/02 21:59 - 04/11/02 20:18	95.4	2.7	0.0
11	3562-4062	04/11/02 21:59 - 09/12/02 20:18	88.4	0.0	0.0
12	4063-4563	09/12/02 21:59 - 13/01/03 20:18	95.0	0.0	0.0
13	4564-5064	13/01/03 21:59 - 17/02/03 20:18	97.4	78.7	78.5
14	5065-5565	17/02/03 21:59 - 24/03/03 20:18	60.7	95.7	95.4
15	5566-6066	24/03/03 21:59 - 28/04/03 20:19	84.6	77.4	75.2
16	6067-6567	28/04/03 21:59 - 02/06/03 20:18	14.0	94.3	94.3
17	6568-7068	02/06/03 21:59 - 07/07/03 20:19	52.9	85.7	84.9
18	7069-7569	07/07/03 21:59 - 11/08/03 20:19	65.1	97.2	97.2
19	7570-8070	11/08/03 21:59 - 15/09/03 20:19	84.0	95.2	94.3
20	8071-8571	15/09/03 21:59 - 20/10/03 20:19	93.6	97.2	96.8
21	8572-9072	20/10/03 21:59 - 24/11/03 20:19	92.6	98.9	98.1
22	9073-9573	24/11/03 21:59 - 29/12/03 20:19	90.6	102.8	102.8
23	9574-10074	29/12/03 21:59 - 02/02/04 20:19	95.0	0.0	0.0
24	10075-10575	02/02/04 21:59 - 08/03/04 20:19	95.2	0.0	0.0
25	10576-11076	08/03/04 21:59 - 12/04/04 20:19	96.6	0.0	0.0
26	11077-11577	12/04/04 21:59 - 17/05/04 20:19	100.0	0.0	0.0
27	11578-12078	17/05/04 21:59 - 21/06/04 20:19	46.3	0.0	0.0
28	12079-12579	21/06/04 21:59 - 26/07/04 20:19	0.0	0.0	0.0
29	12580-13080	26/07/04 21:59 - 30/08/04 20:19	0.0	0.0	0.0

6.2 Quality Flags Monitoring

In this section it is plotted some information contained in the Quality Summary data set of the level 2 products of January. In particular, it is depicted the percentage of flagged points per profile as a function of the first tangent point of every profile for the local species O_3, H_2O, NO_2 and Air. Only

products in dark limb illumination conditions and without fatal errors (error flag in the MPH set to "0") are used.

A profile point in a level 2 product is flagged when:

- The local density is less than a given minimum value
- The local density is greater than a given maximum value
- A negative local density was found
- The line density is not valid. And it occurs when:
    - The acquisition from level 1b is not valid
    - There is no acquisition used for reference star spectrum
    - The line density is less than a given minimum value
    - The line density is greater than a given maximum value
    - A negative line density was found

  For species: air, aerosol, O_3, NO_2, NO_3, OClO
    - No convergence after a given number of LMA iterations
    - χ^2 out of LMA is bigger than χ^2
    - Failure of inversion

  For species: O_2, H_2O
    - Spectro B only: no convergence
    - Spectro B only: data not available
    - Spectro B only: covariance not available

There are points mainly between -35° and +63° latitude because in this period of the year full dark illumination condition occultations (only those products have been used for these plots) are found on that region. In summer, full dark illumination data are mainly in the Southern Hemisphere while in winter it is contrary: full dark illumination occultations are found mainly in the Northern Hemisphere.

Looking at the fig. 6.2-1 the most evident characteristic that can be observed is the high percentage of flagged points per profile for H_2O. Users should not use these data, as their quality is still poor. The percentage of flagged points per profile for O_3 and Air is around 35% whereas for NO_2 it becomes 60%. It can be seen that there are latitudinal bands with almost the same color (same percentages). This means that the percentages of flagged points per profile have a dependence on the stars that have been observed: a given star is always observed at the same latitude but at different longitude.

In fig. 6.2-2 it is depicted the same information as in fig. 6.2-1 but for given specie **valid altitude ranges** (see table 6.2-1), that is, altitude ranges where data with the best quality should be found. For O_3 the percentage of flagged points per profile is small between 20 and 60 km altitude. For NO_2 if becomes less that 20% for altitudes between 20 and 50 km and for Air profiles, the percentage of flagged points is small for altitudes between 25 and 45 km. For H_2O, considering the whole profiles or considering points below 50 km does not change the high percentage of flagged points.

Table 6.2-1: Valid altitude ranges

Specie	O_3	NO_2	Air	H_2O
Valid altitude range (km)	20 - 60	20 - 50	25 - 45	< 50

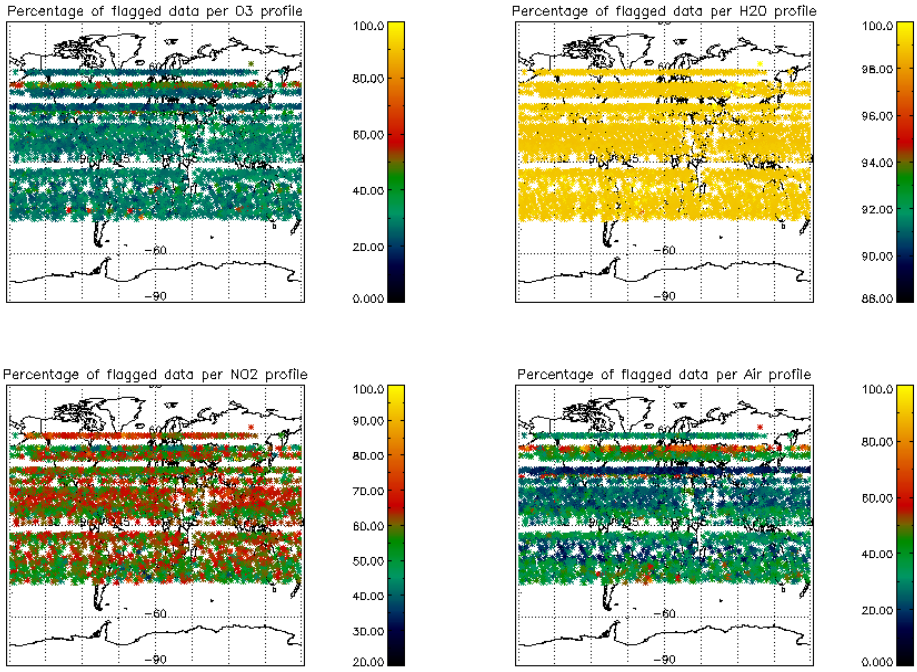

Figure 6.2-1: Percentage of flagged points per profile as a function of the first tangent point of the profile

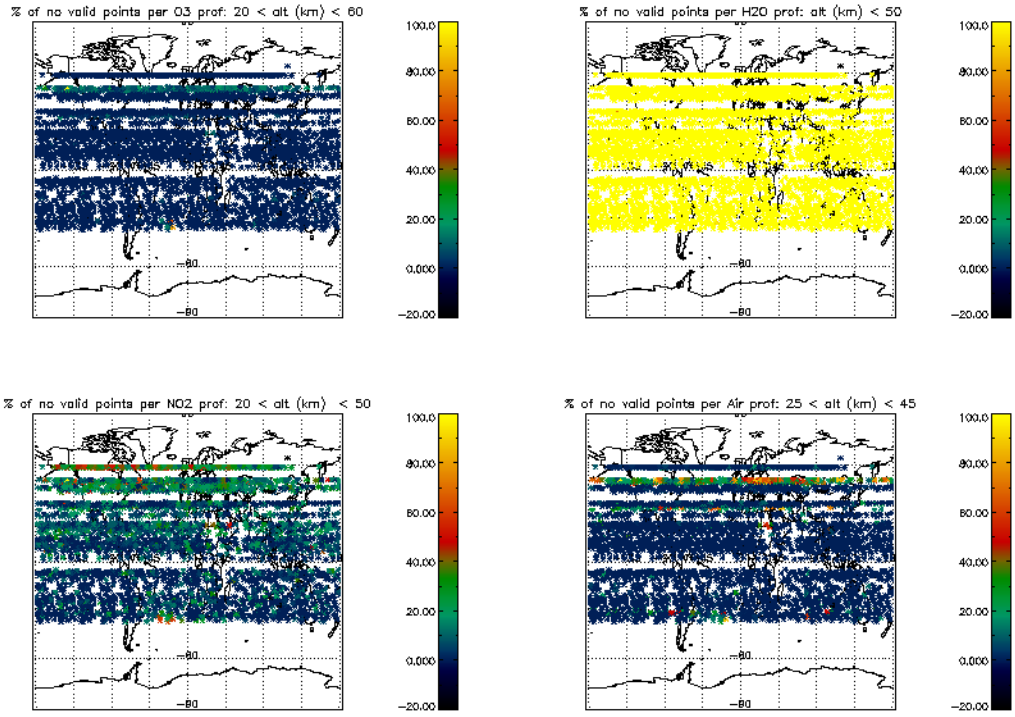

Figure 6.2-2: Same as fig. 6.2-1 but for altitude ranges of table 6.2-1

6.3 Other Level 2 Performance Issues

6.3.1 MONTHLY AVERAGE OF O_3 PROFILES

The plot presented in fig. 6.3-1 is the average of the Ozone values during the reporting month in a grid of 0.5 degrees in latitude per 1 km in altitude. Occultations in dark limb illumination conditions and profiles points that are not flagged have been used. Some known characteristics can be seen:

- O_3 concentrations show a decrease with latitude near 40 km altitude. In the lower latitudes O_3 is generated by photolysis of O_2
- In the middle stratosphere (25-30 km) O_3 is strongly influenced by transport effects. Strong meridional and zonal transport is visible in middle and higher latitudes
- The lower stratosphere shows an O_3 increase with latitude. Highest values can be found within the polar regions due to downward transport of rich air masses

However, other characteristics seem not to be realistic as the values below 15 km, where data are not reliable at the moment.

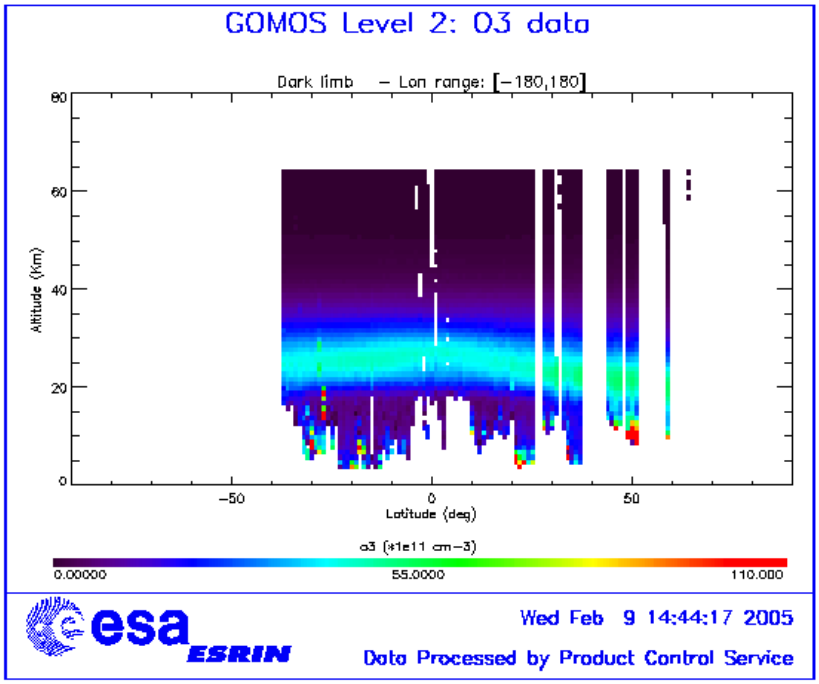

Figure 6.3-1: Average GOMOS O_3 profile during January in a grid of 0.5^o latitude x 1 km altitude

6.3.2 VERTICAL PROFILES MEASURED IN BRIGHT LIMB MODE (GOPR V6.0A)

Although for scientific applications dark limb occultations should be used, we focus in this section on measurements made in bright limb mode, using data retrieved for cycle 022 (orbits between 9073 and 9573, dates between 24/11/2003 and 29/12/2003). The data were processed with GOPR version 60a_60b

(IPF version 5.0), hereafter named v6.0a, including a Tikhonov regularisation, a Global DOAS Inversion on NO2 and on NO3, and a modified budget of the modelling error.

In table 6.3-1 it is presented the number of occultations according to the latitude region, the verticality range, the star magnitude and the star temperature. A fair proportion of occultations are measured at low latitudes (27.0%) and with low "verticality" (i.e. close to the vertical direction) (45.4%). About 40% of measurements are made with cold stars. Most of the measurements come from occultations of weak stars.

Table 6.3-1: Number of occultations of cycle 22 measured in bright limb, categorized for various characteristics

Category	Nb of occultations (cycle22, bright limb)
all	**7241**
low latitudes	**1957 (27.0%)**
mid-latitudes	**3407 (47.0%)**
high latitudes	**1877 (26.0%)**
low "verticality"	**3288 (45.4%)**
mid-"verticality"	**2990 (41.3%)**
high "verticality"	**963 (13.3%)**
cold stars	**2883 (39.8%)**
hot stars	**4358 (60.2%)**
weak stars	**6832 (94.3%)**
strong stars	**409 (5.6%)**

The tangent altitudes at which the stars are lost for vertical profiles are plotted on fig. 6.3-2. Most of the vertical profiles are retrieved down to 20-30km. Some of them are retrieved down to about 5km.

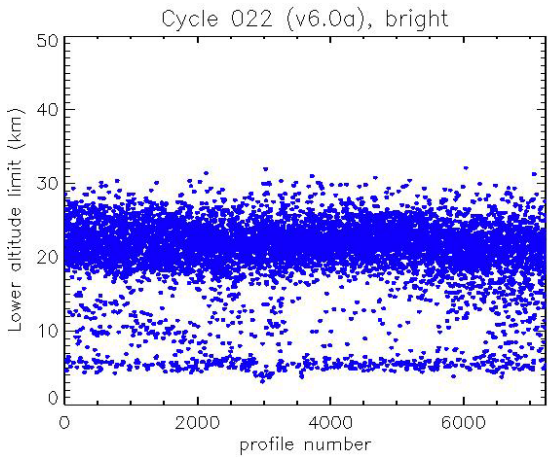

Figure 6.3-2: Values of the lowest altitude (km) of profiles of cycle 22 measured in bright limb mode

Fig. 6.3-3 and 6.3-4 show the relative number of non-flagged local density values per profile (calculated as the percentage of the total number of values of each profile) for O_3, NO_2, NO_3, O_2, air, H_2O. For H_2O,

only values at altitudes lower than 50km are considered (no non-flagged H_2O value is provided at higher altitudes). For O_3 profiles, the categories with the highest number of profiles are 30% to 40%, and 40% to 50% of non-flagged values per profile. For NO_2, most of the profiles show a relative number of non-flagged values between 10% and 30%, and for NO_3, between 20% and 30%. For O_2 profiles, the category with the highest number of profiles is 0% to 10% of non-flagged values (for about 40% of the profiles). For air profiles, the largest number of profiles is obtained for categories between 30% and 40%, and between 40% and 50%. For H_2O profiles below 50km, more than 80% of the profiles have a number of non-flagged values lower than 10%. It is to be noted that a large number of them have no non-flagged value at all.

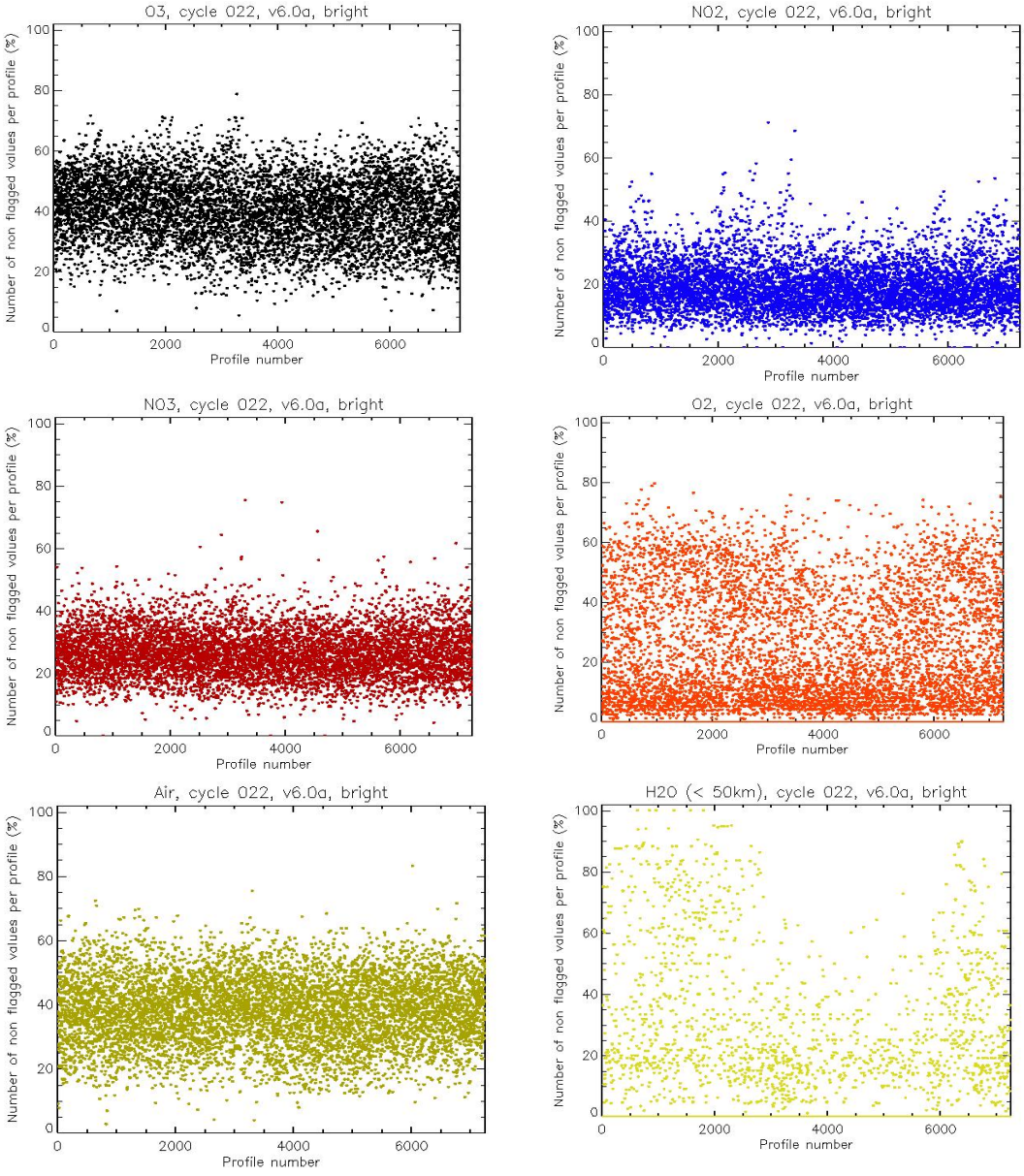

Figure 6.3-3: Relative number of non-flagged values of local density for measurements of cycle 22 made in bright limb mode, calculated for each profile as the percentage of the total number of values of the profile

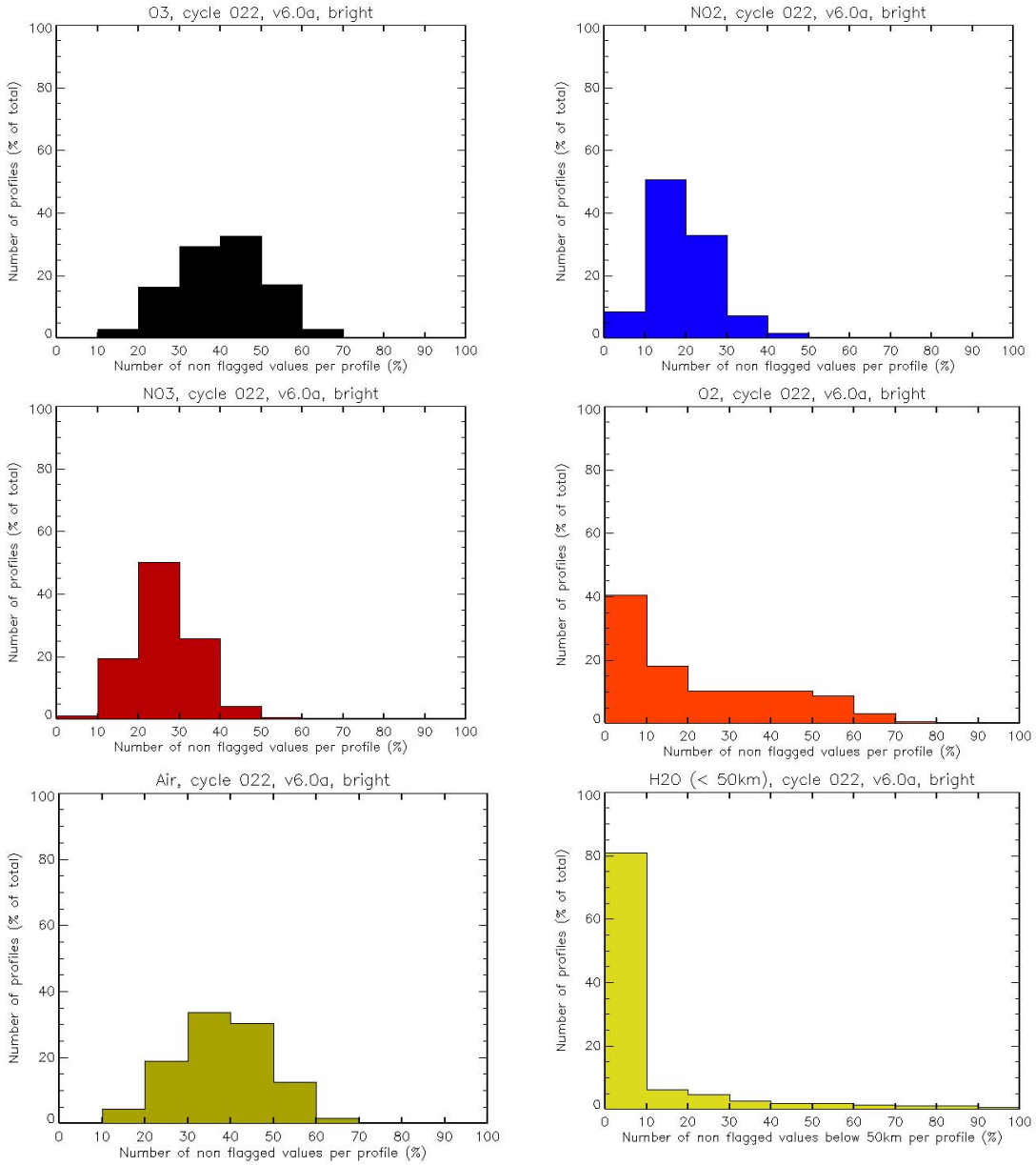

Figure 6.3-4: Histograms of the relative number of non-flagged values of local density for measurements of cycle 22 made in bright limb mode, calculated for each profile as the percentage of the total number of values of the profile. The number for each class is the relative number of profiles, calculated as the percentage of the total number of profiles

Fig. 6.3-5 shows the values of the column density and of the local density of O_3, NO_2, NO_3 and H_2O for 200 occultations of cycle 22 measured in bright limb mode. Only non flagged values are plotted. For these occultations, O_3 profiles show a high dispersion of the column density values. Below 30km, non-flagged values of the local density are sparse and noisy for many of them. For NO_2 and NO_3 profiles, the same features may be observed, with a higher dispersion of the values of local density at high altitudes, especially for NO_3. There are only a few non-flagged values for H_2O vertical profiles below 50km, even for the column density, and many of them show high dispersion. The dispersion of the values for the different species is mainly due to the inaccuracy of the background correction of the target band (the band containing the star signal) in the Level1b processing.

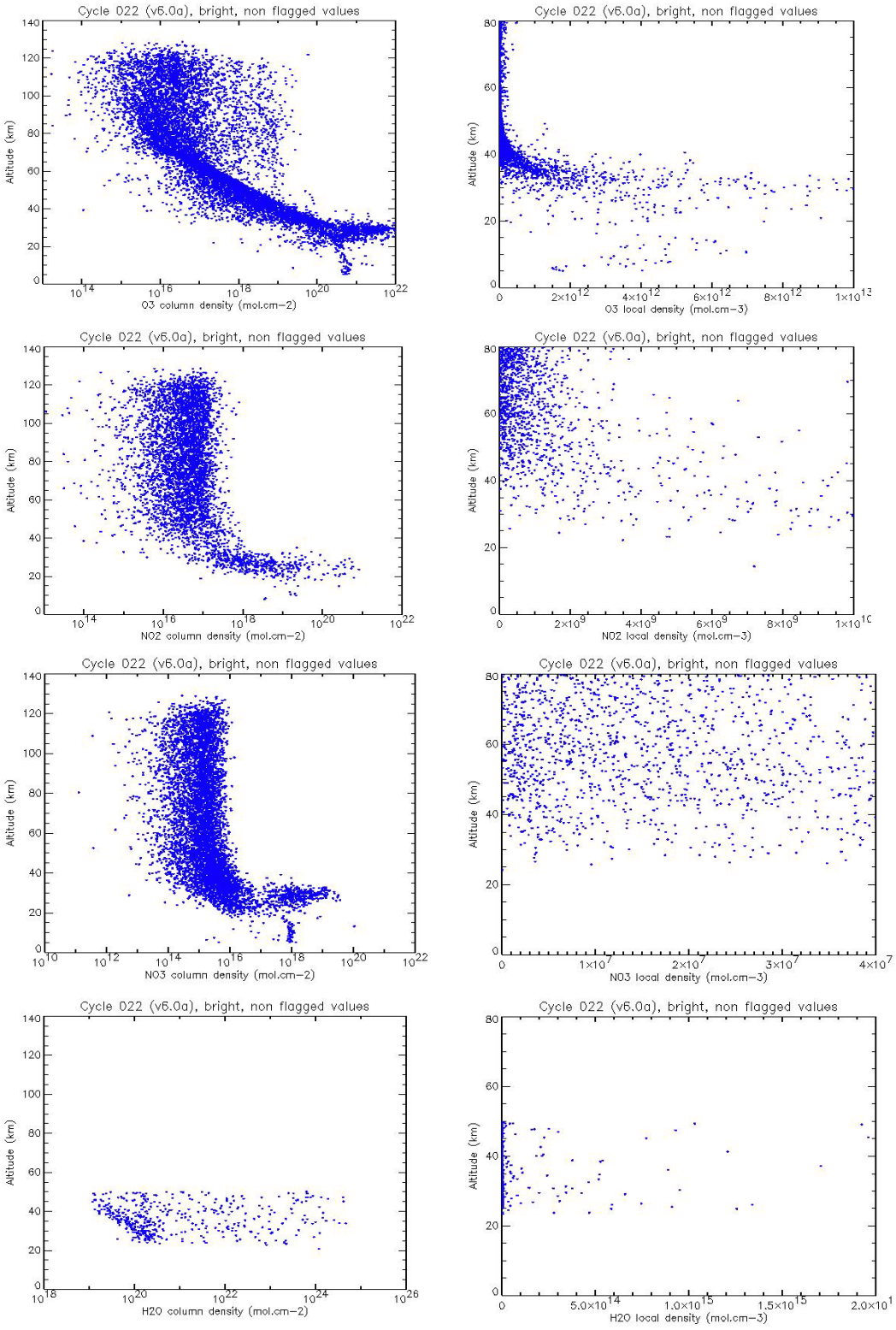

Figure 6.3-5: Values of column densities (left) in molec cm^{-2} between 0 and 140km altitude and local densities (right) in molec cm^{-3} between 0 and 80km altitude. Only non-flagged values are plotted

Basing on the results from these 200 occultations, the Level 2 products of bright limb occultations may provide valid data, but further improvement of the retrieval processes should be required before using all bright limb products. A modified version of GOPR, 6.0b6.0c, is currently under testing. It includes two main modifications: the number of DOAS loops is now limited thanks to a modified χ^2-convergence criteria; and the negative column densities are not flagged anymore. The impact of these updates will be presented in future reports, but we do not anticipate major changes in the dispersion or the irrelevancy of some of the density values obtained in bright limb. The main issue in the retrieval of the bright limb occultations is the inaccuracy of the background correction of the target band in the Level1b processing.

7 VALIDATION ACTIVITIES AND RESULTS

7.1 Inter-Comparison with external data

7.1.1 GOMOS-ECMWF COMPARISONS: TEMPERATURE AND OZONE

Due to restrictions in the current METEO product format, filtering of METEO data is not possible. ECMWF results are therefore partially based on data that are not to be used for scientific application, as mentioned in the disclaimer (http://envisat.esa.int/dataproducts/availability/disclaimers)

Summary of ECMWF GOMOS monthly report for January data (GOM_RR__2P):

- No GOMOS temperature/ozone data from 25 January onwards.
- GOMOS temperature/ozone data gap between about 10S-30N and 30E-100E for most of the levels/layers has been reduced.
- Very few temperature/ozone data in the latitudinal bands between 0 and 5S and around 40N and 40S.
- Overall good agreement between GOMOS and ECMWF temperatures.
- GOMOS temperatures are lower than ECMWF temperatures in most of the stratosphere and mesosphere, but area mean departures are less than 1% in most of the stratosphere. Larger departures are found in the mesosphere in particular at the model top.
- Large differences between GOMOS and ECMWF ozone values (over 50% in places).
- Large scatter of GOMOS ozone data.
- Scatter plots still show some unrealistically low GOMOS ozone values.
- No water vapor data in NRT GOMOS BUFR files.
- The monitoring statistics for January were produced with the operational ECMWF model, CY28R4.

The full January ECMWF report can be found in the link below:
http://earth.esa.int/pcs/envisat/tmp_calval_res/2005/ecmwf_gomos_monthly_200501_all.pdf

7.1.2 ENVISAT QUALITY ASSESSMENT WITH LIDAR (EQUAL)

Summary of the annual EQUAL project report for 2004:
The project supports and performs the quality assessment of ozone and temperature profiles retrieved from ENVISAT data using lidar data. In total eleven lidar stations are part of the EQUAL network and

they have submitted in HDF-format over 2000 profiles to the correlative database, which is maintained by NILU in Norway. The availability of ENVISAT data suitable for validation has been quite limited. For MIPAS, we had no data available but this situation will improve in 2005 as data can now be downloaded by ftp and data are processed by IMK in Karlsruhe. For SCIAMACHY, there was no official data product and we resided to data from IFE in Bremen, but these data reached us at the end of 2004 and have not yet been analyzed. In 2005 the situation will improve, as official ESA offline data products are now becoming available through ftp. For GOMOS, we now regularly receive official ESA data via CD-ROM. From these data we could use data generated after September 2004 which reached us at the end of 2004. Data processed with ESA's prototype processor at ACRI were available covering the period July 2002 until April 2003. These data have been extensively validated and results were presented at several conferences and in scientific journals. In dark limb the GOMOS data agree very well with the correlative data, and between 14 and 64 km altitude their differences only show a small (2.5–7.5%) insignificant negative bias with a standard deviation of 11–16% (19–63 km). This conclusion was demonstrated to be independent of the star temperature and magnitude and the latitudinal region of the GOMOS observation, with the exception of a slightly larger bias in the Polar Regions at altitudes between 35 and 45 km.

The full 2004 annual EQUAL report can be found in the link below:
http://earth.esa.int/pcs/envisat/tmp_calval_res/2004/EQUAL_Annual_Report_2004.pdf

7.1.3 TECHNICAL ASSISTANCE TO ENVISAT ATMOSPHERIC CHEMISTRY VALIDATION (TASTE)

Summary of the annual TASTE project report for 2004:
The TASTE project provides ESA with Technical Assistance to ENVISAT atmospheric chemistry validation throughout the satellite lifetime. The project involves an international consortium gathering complementary expertise in remote sensing and satellite validation, namely, BIRA-IASB (Belgium), CNRS/SA (France), FMI-ARC (Finland), IFE/Bremen (Germany), IMK/FZK (Germany), INTA (Spain), KMI-IRM (Belgium), KNMI (Netherlands), NIWA (New Zealand), and SPbSU (Russia), and their collaborators. Main tasks relate to the collection and delivery of correlative data to the ENVISAT Cal/Val database operated at NILU on behalf of ESA, the monitoring of those data sets, geophysical validation studies based on comparisons between ENVISAT (GOMOS, MIPAS and SCIAMACHY) and ground-based data sets, and the valorization of the validation results.
The document reports on activities carried out in the first term of ESA TASTE project. Section B reviews the provision of correlative data records. Section C gives an overview of the validation work performed during the reporting period and to which members of the consortium have contributed. Section D reports on the valorization of the correlative data and of the validation results. Section E concludes with the perspectives for next term.

The full 2004 annual TASTE report can be found in the link below:
http://earth.esa.int/pcs/envisat/tmp_calval_res/2004/TASTE_Annual_Report_2004.pdf

7.2 GOMOS-Climatology comparisons (N/A for this month)

Results will be presented upon availability.

7.3 GOMOS Assimilation (N/A for this month)

Results will be presented upon availability.

7.4 Consistency Verification: GOMOS-GOMOS Inter-comparison (N/A for this month)

Results will be presented upon availability.